Received: 10 October 2016 | Revised: 9 October 2017 | Accepted: 10 October 2017

DOI: 10.1002/cne.24344

RESEARCH ARTICLE

WILEY The Journal of Comparative Neurology

Transmitter receptors reveal segregation of the arcopallium/amygdala complex in pigeons (*Columba livia*)

Christina Herold[1] | Christina Paulitschek[1] | Nicola Palomero-Gallagher[2] | Onur Güntürkün[3] | Karl Zilles[2,4]

[1]C. and O. Vogt Institute of Brain Research, Medical Faculty, Heinrich-Heine University of Düsseldorf, Düsseldorf, Germany

[2]Institute of Neuroscience and Medicine INM-1, Research Center Jülich, Jülich, Germany

[3]Department of Biopsychology, Institute of Cognitive Neuroscience, Faculty of Psychology, Ruhr-University Bochum, Bochum, Germany

[4]Department of Psychiatry, Psychotherapy and Psychosomatics, RWTH Aachen University, and JARA – Translational Brain Medicine, Aachen, Germany

Correspondence
Christina Herold, C. & O. Vogt-Institute of Brain Research, University of Düsseldorf, Düsseldorf 40225, Germany.
Email: christina.herold@uni-duesseldorf.de

Funding information
Grant sponsor: Deutsche Forschungsgemeinschaft, Grant No.: SFB 1280 (O.G.).

Abstract

At the beginning of the 20th century it was suggested that a complex group of nuclei in the avian posterior ventral telencephalon is comparable to the mammalian amygdala. Subsequent findings, however, revealed that most of these structures share premotor characteristics, while some indeed constitute the avian amygdala. These developments resulted in 2004 in a change of nomenclature of these nuclei, which from then on were named arcopallial or amygdala nuclei and referred to as the arcopallium/amygdala complex. The structural basis for the similarities between avian and mammalian arcopallial and amygdala subregions is poorly understood. Therefore, we analyzed binding site densities for glutamatergic AMPA, NMDA and kainate, GABAergic $GABA_A$, muscarinic M_1, M_2 and nicotinic acetylcholine (nACh; $\alpha_4\beta_2$ subtype), noradrenergic α_1 and α_2, serotonergic 5-HT_{1A} and dopaminergic $D_{1/5}$ receptors using quantitative in vitro receptor autoradiography combined with a detailed analysis of the cyto- and myelo-architecture. Our approach supports a segregation of the pigeon's arcopallium/amygdala complex into the following subregions: the arcopallium anterius (AA), the arcopallium ventrale (AV), the arcopallium dorsale (AD), the arcopallium intermedium (AI), the arcopallium mediale (AM), the arcopallium posterius (AP), the nucleus posterioris amygdalopallii pars basalis (PoAb) and pars compacta (PoAc), the nucleus taeniae amgygdalae (TnA) and the area subpallialis amygdalae (SpA). Some of these subregions showed further subnuclei and each region of the arcopallium/amygdala complex are characterized by a distinct multi-receptor density expression. Here we provide a new detailed map of the pigeon's arcopallium/amygdala complex and compare the receptor architecture of the subregions to their possible mammalian counterparts.

KEYWORDS

amygdala, arcopallium, avian, autoradiography, receptor, RRID:SCR_013566, RRID:SCR_001905, RRID:SCR_015627

Abbreviations: A, Arcopallium; AA, Arcopallium anterius; ACh, Acetylcholine; AD, Arcopallium dorsale; ADl, Arcopallium dorsale pars lateralis; ADm, Arcopallium dorsale pars medialis; ADp, Arcopallium dorsale pars posterior; AI, Arcopallium intermedium; AId, Arcopallium intermedium pars dorsalis; AIv, Arcopallium intermedium pars ventralis; AIvm, Arcopallium intermedium pars ventromedialis; AM, Arcopallium mediale; AMm, Arcopallium mediale pars magnocellularis; AMp, Arcopallium mediale pars parvocellularis; AMPA, α-amino-3-hydroxy-5-methyl-4-isoxazolepropionic acid; AP, Arcopallium posterioris; AV, Arcopallium ventrale; AVm, Arcopallium ventrale pars medialis; BSTL, Bed nucleus of the Stria Terminalis, pars lateralis; CDL, Area corticoidea dorsolateralis; CPi, Cortex piriformis; DA, Tractus dorso-arcopallialis; FA, Tractus fronto-arcopallialis; GABA, γ-Amino-butyric acid; GP, Globus pallidus; HF, Hippocampal formation; LAD, Lamina arcopallialis dorsalis; LSt, Lateral striatum; M, Mesopallium; N, Nidopallium; NCL, Nidopallium caudolaterale; NCVl, Nidopallium caudoventrale pars lateralis; NMDA, N-Methyl-D-aspartic acid; PoA, Nucleus posterioris amygdalopallii; PoAb, Nucleus posterioris amygdalopallii pars basalis; PoAc, Nucleus posterioris amygdalopallii pars compacta; SpA, Area subpallialis amygdalae; ST, Striatum; TnA, Nucleus taeniae amygdalae; TPO, Area temporo-parieto-occipitalis; V, Ventricle.

1 | INTRODUCTION

New concepts of vertebrate brain evolution resulted recently in a better understanding of the organization of the avian telencephalon (Jarvis et al., 2005; Reiner et al., 2004). Furthermore, in the last couple of years, novel but conflicting hypotheses on homologies of avian and mammalian pallial structures and cell types have been claimed and new genetic models were developed (Belgard et al., 2013; Butler, Reiner, & Karten, 2011; Chen, Winkler, Pfenning, & Jarvis, 2013; Dugas-Ford, Rowell, & Ragsdale, 2012; Jarvis et al., 2013; Karten, 2015; Puelles, 2011; Vicario, Abellán, Desfilis, & Medina, 2014). Beside the known homologies of brain regions that are based on the same developmental origin, some regions also share anatomical and molecular traits, which seem to be a result of convergent evolution based on functional specialization (Güntürkün & Bugnyar, 2016; Herold, Coppola, & Bingman, 2015; Herold, Joshi, Chehadi, Hollmann, & Güntürkün, 2012; Herold et al., 2011; Pfenning et al., 2014). One region that has been intensely discussed in this context is the avian arcopallium/amygdaloid complex. According to the old and outdated nomenclature (Karten & Hodos, 1967), this ventrolateral part of the posterior telencephalon was called archistriatum and was suggested to be partly comparable to the mammalian amygdala (Zeier & Karten, 1971). However, evidence from neurochemical, developmental, and behavioral data showed that most parts of the archistriatum are largely of premotor nature (Butler et al., 2011; Kuenzel, Medina, Csillag, Perkel, & Reiner, 2011; Reiner et al., 2004; Yamamoto, Sun, Wang, & Reiner, 2005). Accordingly, these premotor areas were termed arcopallium in the new nomenclature while the remaining subnuclei were assumed to constitute the amygdala (Reiner et al., 2004). In mammals, the amygdala is also a complex structure, with multiple subnuclei, and various neuronal subtypes and connections. Similarly, developmental and genetic studies have confirmed that both the avian and the mammalian amygdala complexes share several expression profiles of specific markers (Dugas-Ford et al., 2012; Jarvis et al., 2013; Kuenzel et al., 2011; Montiel & Molnar, 2013; Moreno & Gonzalez, 2007; Pfenning et al., 2014; Puelles et al., 2015; Vicario et al., 2014; Vicario, Abellán, & Medina, 2015). Not only genetic but also connectional analyses demonstrate that the premotor subregions of the arcopallium share similar connectivity patterns as the mammalian premotor areas, while the limbic nuclei showed comparable connections to parts of the mammalian amygdala (Atoji & Wild, 2012; Güntürkün & Bugnyar, 2016; Hanics, Teleki, Alpar, Szekely, & Csillag, 2016; Reiner et al., 2004; Shanahan, Bingman, Shimizu, Wild, & Güntürkün, 2013; Zeier & Karten, 1971). This is also true for functional, pharmacological and electrophysiological studies in various bird species that make it likely that the avian arcopallium/amygdaloid complex is constituted by diverse subregions that have either premotor or limbic functions and participate in visual, vocal, auditory, and emotional learning, fear and reproduction behavior as well as neuroendocrine control and homeostasis (Campanella et al., 2009; Cohen, 1975; Cross et al., 2013; da Silva et al., 2009; Dafters, 1975; Kuenzel et al., 2011; Pfenning et al., 2014; Saint-Dizier et al., 2009; Scarf, Stuart, Johnston, & Colombo, 2016; Whitney et al., 2014; Winkowski & Knudsen, 2007). However, the heterogeneity of this region constitutes a major challenge to understand the functional organization and evolutionary origin of the arcopallium/amygdala complex in birds (Medina & Abellán, 2009). In addition, a common consensus of homologies between birds and mammals is still missing.

Since the expression of multiple transmitter receptors in the brain has been proven as a powerful tool to delineate different areas, and to identify similarities among regions between various mammalian species (Palomero-Gallagher, Zilles, Schleicher, & Vogt, 2013; Vogt et al., 2013; Zilles, 2005; Zilles & Palomero-Gallagher, 2016) and also between birds and mammals (Herold et al., 2015; Herold et al., 2011; Jarvis et al., 2013; Kubikova, Wada, & Jarvis, 2010; Lovell, Clayton, Replogle, & Mello, 2008; Sun & Reiner, 2000; Wada, Sakaguchi, Jarvis, & Hagiwara, 2004), we analyzed the neurotransmitter receptor-, myelo- and cellular-architecture of the pigeon's arcopallium/amygdala complex. The resulting detailed map of this region can be used as a basis for comparisons to the mammalian amygdala complex and cortical areas in the future.

2 | MATERIAL AND METHODS

2.1 | Receptor autoradiography and histology

We examined six adult pigeon brains (*Columba livia*) of unknown sex. Animals were obtained from local breeders and were housed in individual cages (30 × 30 × 45 cm) at 21 ± 1°C temperature and in a humidity controlled room with a 12-hr light/dark circle. The birds had free access to grit, food and water ad libitum. All experimental procedures were approved by the national authority (LANUV NRW, Germany) and were carried out in accordance with the National Institute of Health Guide for Care and Use of Laboratory Animals. Animals were decapitated, brains were removed from the skull, frozen immediately in isopentane at −40°C and stored at −70°C. Serial coronal 10 μm sections were cut with a cryostat microtome (2800 Frigocut E, Reichert-Jung). Sections were thaw-mounted on gelatinized glass slides, freeze-dried and stained with a modified cell body staining or Gallyas myelin staining (Gallyas, 1971; Merker, 1983) for cyto- and myelo-architectonic analysis, or processed for receptor autoradiography.

Details of the autoradiographic labeling procedure have been published elsewhere (Herold et al., 2014; Zilles, Palomero-Gallagher, et al., 2002; Zilles, Schleicher, Palomero-Gallagher, & Amunts, 2002). Binding protocols are summarized in Table 1. Three steps were performed in the following sequence:

1. A preincubation step removed endogenous ligand from the tissue.
2. During the main incubation step binding sites were labeled with the respective tritiated ligand (total binding), or co-incubated with the tritiated ligand and a 1,000–10,000-fold excess of specific non-labeled ligand (displacer) determined non-displaceable, and thus, non-specific binding. Specific binding is the difference between total and non-specific binding. It was less than 5% in all cases.
3. A final rinsing step eliminated unbound radioactive ligand from the sections.

The following binding sites were labeled according to the above cited protocols: (a) α-amino-3-hydroxy-5-methyl-4-isoxalone propionic acid (AMPA) receptor with [^{3}H] AMPA, (b) kainate receptor with [^{3}H]kainate, (c) *N*-methyl-D-aspartate (NMDA) receptor with [^{3}H]MK-801, (d) γ-aminobutyric acid A ($GABA_A$) receptor with [^{3}H]muscimol, (e) muscarinic cholinergic M_1 receptor with [^{3}H]pirenzepine, (f) muscarinic cholinergic M_2 receptor with [^{3}H]oxotremorine-M, (g) nicotinic cholinergic (nACh; $\alpha_4\beta_2$ subtype) receptor with [^{3}H]cytisine, (h) noradrenergic α_1 adrenoreceptor with [^{3}H]prazosin, (i) noradrenergic α_2 adrenoreceptor with [^{3}H]RX-821002, (j) serotonergic 5-HT_{1A} receptor with [^{3}H]8-OH-DPAT, and (k) dopaminergic $D_{1/5}$ receptors with [^{3}H]SCH 23390. Sections were air-dried overnight and subsequently co-exposed for 4–5 weeks against a tritium-sensitive film (Hyperfilm, Amersham, Braunschweig, Germany, RRID:SCR_013566) with plastic [^{3}H]-standards (Microscales, Amersham) of known concentrations of radioactivity.

2.2 | Image analysis

The resulting autoradiographs were subsequently processed using densitometry with a video-based image analyzing technique (Zilles, Schleicher, et al., 2002). Autoradiographs were digitized by means of a KS-400 image analyzing system (Kontron, Germany) connected to a CCD camera (Sony, Japan) equipped with a S-Orthoplanar 60-mm macro lens (Zeiss, Germany). The images were stored as binary files with a resolution of 512 × 512 pixels and 8-bit gray value. The gray value images of the co-exposed microscales were used to compute a calibration curve by nonlinear, least-squares fitting, which defined the relationship between gray values in the autoradiographs and concentrations of radioactivity. This enabled the pixel-wise conversion of the gray values of an autoradiograph into the corresponding concentration of radioactivity. The concentrations of binding sites occupied by a ligand under incubation conditions are transformed into fmol/mg protein at saturation conditions by means of the equation: $(K_D + L)/A_S \times L$, where K_D is the equilibrium dissociation constant of ligand-binding kinetics, L is the incubation concentration of ligand, and A_S the specific activity of the ligand. The results of these calculations were used for binding site density measurements. The digitized autoradiographic images were color-coded only to facilitate the detection of regional differences in binding site densities by visual inspection.

2.3 | Anatomical identification

The borders of the arcopallium/amygdala complex and its subregions were identified based on our cyto-, myelo- and receptor-architectonic data, and previous cytoarchitectural, neurochemical, tract-tracing, and imaging studies (Atoji, Saito, & Wild, 2006; Atoji & Wild, 2009; H. Karten & Hodos, 1967; Kröner & Güntürkün, 1999; Reiner et al., 2004; Shanahan et al., 2013; Yamamoto & Reiner, 2005; Zeier & Karten, 1971). Borders of the different subregions were traced on prints of the digitized autoradiographs by projecting the cell body and the myelin stained sections onto the digitized images of the autoradiographs between anterior–posterior levels A 7.75 and A 4.50 according to the atlas of Karten and Hodos (1967). The mean of the concentration of each binding site (fmol/mg protein) in each subregion of the arcopallium/amygdala complex was calculated over the sampled anterior-posterior levels from each animal, averaged across the six animals, and is reported as the overall receptor concentration (mean ± standard error of mean (*SEM*)). Quantitative, multi-receptor data are presented in color-coded autoradiographs and in regional fingerprints that are prepared as polar plots or histograms that separately show the density for the receptors in each subregion.

2.4 | Statistical analysis

To determine differences in receptor densities among subregions and adjacent structures we compared the main subregions of the arcopallium/amygdala complex and included also the lateral division of the nidopallium caudoventrale (NCVl). To do so, we first applied a Friedman ANOVA across all subregions for each ligand (Table 2). If significant, pair-wise comparisons were run with the Wilcoxon-rank test (Table 3). Differences between intra-nuclear substructures were directly analyzed with Wilcoxon-rank tests. For the general statistical analyses, Statistica 10 (StatSoft, Tulsa, RRID:SCR_015627) was used. The significance level was set at 0.05. Further, a hierarchical cluster analysis was carried out to detect putative groupings of areas according to the degree of (dis) similarity of their receptor architecture (Palomero-Gallagher et al., 2009). The Euclidean distance was applied as a measure of (dis)similarity since it takes both differences, the size and the shape of receptor fingerprints into account, and the Ward linkage algorithm as the linkage method. This combination yielded the maximum cophenetic correlation coefficient as compared to any combination of alternative linkage methods and measurements of (dis)similarity. Prior to this analysis, the densities of each receptor type were transformed to *z*-scores across all areal densities of that specific receptor, thus ensuring an equal weighting of each receptor without eliminating relative differences in receptor densities among areas. The hierarchical cluster analysis was carried out with in house R-scripts (R Foundation for Statistical Computing, http://www.r-project.org, RRID:SCR_001905).

3 | RESULTS

3.1 | Qualitative analysis of the cyto- and myeloarchitecture of the arcopallium/amygdala complex

Figure 1 shows the arcopallium/amygdala complex in a Nissl (a)- and a myelin (b)-stained transverse section of a pigeon brain at the anterior–posterior coordinate A 6.50 (Karten & Hodos, 1967) and a magnification of the region of interest (1c) clipped from the Nissl image in Figure 1a. For a more detailed overview, different atlas levels are shown in representative coronal cell body- and myelin-stained sections depicting the outlines of the arcopallium/amgydala complex and surrounding structures in Figure 2 (a–l; Nissl) and Figure 3 (a–l; myelin) that were used as an orientation for the identification of subregions in the receptor autoradiographs. Thereby, the boundaries to map the different arcopallium/amygdala subdivisions followed previous cytoarchitectural, neurochemical, tract-tracing, and imaging studies (Atoji et al., 2006;

TABLE 1 Incubation conditions used for receptor autoradiography

Receptor	[^{3}H] ligand (incubation concentration)	Displacer (incubation concentration)	Incubation buffer	Preincubation step	Main incubation step	Rinsing step
glutamatergic AMPA	[^{3}H] AMPA (10 nM)	Quisqualate (10 μM)	50 mM Tris-acetate (pH 7.2)	3 × 10 min at 4°C in incubation buffer	45 min at 4°C in incubation buffer + 100 mM KSCN	4 × 4 s at 4°C in incubation buffer + 2 × 2 s at 4°C in acetone/glutaraldehyde
glutamatergic Kainate	[^{3}H] kainate (8 nM)	Kainate (100 μM)	50 mM Tris-citrate (pH 7.1)	3 × 10 min at 4°C in incubation buffer	45 min at 4°C in incubation buffer + 10 mM Ca-acetate	4 × 4 sec at 4°C in incubation buffer + 2 × 2 sec at 4°C in acetone/glutaraldehyde
glutamatergic NMDA	[^{3}H] MK-801 (5 nM)	MK-801 (100 μM)	50 mM Tris-HCl (pH 7.2)	15 min at 25°C in incubation buffer	60 min at 25°C in incubation buffer + 30 μM glycine + 50 μM spermidine	2 × 5 min at 4°C in incubation buffer
muscarinic cholinergic M_1	[^{3}H] pirenzepine (1 nM)	Pirenzepine (10 μM)	Modified Krebs-Ringer buffer (pH 7.4)	20 min at 25°C in incubation buffer	60 min at 25°C in incubation buffer	2 × 5 min at 4°C in incubation buffer
muscarinic cholinergic M_2	[^{3}H] oxotremorine-M (0.8 nM)	Carbachol (1 μM)	20 mM Hepes-Tris (pH 7.5) + 10 mM $MgCl_2$	20 min at 25°C in incubation buffer	60 min at 25°C in incubation buffer	2 × 2 min at 4°C in incubation buffer
nicotiniccholinergic $\alpha_4\beta_2$	[^{3}H] cytisine (1 nM)	Nicotine (10 μM)	50 mM Tris–HCl (pH 7.4) + 120 mM NaCl + 5 mM KCl + 1 mM MgCl2 + 2.5 mM CaCl2	15 min at 22 °C in incubation buffer	90 min at 4°C in incubation buffer	2 × 2 min at 4°C in incubation buffer
adrenergic α_1	[^{3}H] prazosin (0.2 nM)	Phentolamine (10 μM)	50 mM Tris-HCl (pH 7.4)	30 min at 37°C in incubation buffer	45 min at 30°C in incubation buffer	2 × 5 min at 4°C in incubation buffer
adrenergic α_2	[^{3}H] RX-821002 (6nM)	(-) adrenaline (10μM)	50 mM Tris-HCl (pH 7.4) + 100 mM $MnCl_2$ +0.1% Ascorbic acid +0.3 μM 8-OH-DPAT	30 min at 22°C in incubation buffer	30 min at 22°C in incubation buffer	2 × 20 s at 4°C in incubation buffer
GABAergic $GABA_A$	[^{3}H] muscimol (6 nM)	GABA (10 μM)	50 mM Tris-citrate (pH 7.0)	3 × 5 min at 4°C in incubation buffer	40 min at 4°C in incubation buffer	3 × 3 s at 4°C in incubation buffer
serotoninergic $5\text{-}HT_{1A}$	[^{3}H] 8-OH-DPAT (1 nM)	Serotonin (10 μM)	170 mM Tris-HCl (pH 7.6)+4 mM $CaCl_2$ +0.01% Ascorbic acid	30 min at 22°C in incubation buffer	60 min at 22°C in incubation buffer	1 × 5 min at 4°Cin incubation buffer
dopaminergic $D_{1/5}$	[^{3}H] SCH-23390 (0.5nM)	SKF 83566 (1μM)	50 mM Tris-HCl (pH 7.4) + 120 mM NaCl + 5 mM KCl + 2 mM $CaCl_2$ + 1 mM $MgCl_2$ + 1 μM Mianserin	20 min at 22°C in incubation buffer	90 min at 22°C in incubation buffer	2 × 10 min at 4°C in incubation buffer

TABLE 2 Neurotransmitter receptor densities (fmol/mg protein) in different subregions of the arcopallium/amygdala complex, the nidopallium caudale ventro-laterale and the posterior lateral striatum (mean ± *SEM*) and results of the Friedman ANOVA displaying regional differences for all subregions for each receptor type (all $N = 6$, df = 10; LSt not included)

Subregion/ Receptor	AA	AD	AM	AI	AV	AP	PoAb	PoAc	TnA	SpA	NCVI	LSt	Friedman ANOVA (χ^2)
AMPA	1325 ± 133	1551 ± 101	1601 ± 62	1534 ± 77	1722 ± 87	1651 ± 85	1264 ± 93	1610 ± 105	1403 ± 164	1147 ± 100	1554 ± 98	1438 ± 47	28.82**
Kainate	774 ± 160	323 ± 30	275 ± 35	362 ± 35	796 ± 81	266 ± 26	316 ± 39	333 ± 18	225 ± 38	636 ± 37	256 ± 30	878 ± 41	43.21***
NMDA	1238 ± 248	1330 ± 52	1338 ± 29	1234 ± 51	1690 ± 79	1478 ± 75	1359 ± 126	1685 ± 107	1133 ± 58	741 ± 54	1589 ± 78	1205 ± 50	44.52***
$GABA_A$	906 ± 196	535 ± 50	414 ± 48	654 ± 60	677 ± 63	402 ± 40	361 ± 43	577 ± 76	332 ± 34	578 ± 48	605 ± 86	1539 ± 76	43.82***
M_1	107 ± 20	172 ± 11	64 ± 11	115 ± 10	42 ± 3	48 ± 5	54 ± 15	61 ± 4	27 ± 7	56 ± 12	42 ± 9	78 ± 11	43.21***
M_2	235 ± 42	359 ± 34	200 ± 17	324 ± 33	129 ± 17	185 ± 25	98 ± 16	142 ± 18	206 ± 25	327 ± 47	151 ± 36	390 ± 39	45.67***
$\alpha_4\beta_2$	41 ± 2	41 ± 3	47 ± 1	41 ± 2	58 ± 4	62 ± 6	52 ± 3	69 ± 4	72 ± 3	57 ± 5	51 ± 5	59 ± 4	40.00***
α_1	13 ± 4	17 ± 2	14 ± 2	10 ± 1	11 ± 1	10 ± 4	10 ± 2	110 ± 16	7 ± 2	13 ± 2	78 ± 5	14 ± 2	37.36***
α_2	231 ± 32	270 ± 20	247 ± 7	221 ± 6	121 ± 9	590 ± 130	233 ± 17	254 ± 14	831 ± 49	415 ± 27	206 ± 38	347 ± 20	41.67***
$5\text{-}HT_{1A}$	86 ± 22	64 ± 4	54 ± 5	96 ± 8	77 ± 5	41 ± 6	40 ± 5	99 ± 13	43 ± 3	40 ± 4	65 ± 8	34 ± 2	41.55***
$D_{1/5}$	41 ± 18	22 ± 1	19 ± 2	20 ± 2	16 ± 1	26 ± 4	14 ± 1	35 ± 4	14 ± 1	16 ± 1	33 ± 5	41 ± 2	35.76***

*$p < .05$, **$p < .01$, ***$p < .001$. Abbreviations see list.

Atoji & Wild, 2009; H. Karten & Hodos, 1967; Kröner & Güntürkün, 1999; Reiner et al., 2004; Shanahan et al., 2013; Yamamoto & Reiner, 2005; Zeier & Karten, 1971) and our own analysis. Beginning at anterior positions and moving posteriorly, we subdivided the arcopallium into the following divisions: the arcopallium anterius (AA), the arcopallium ventrale (AV), the arcopallium dorsale (AD), the arcopallium intermedium (AI), the arcopallium mediale (AM), and the arcopallium posterius (AP). AA, the anterior tip of the arcopallium, is the beginning of a spherical structure that is encompassed dorsally by the tractus fronto-arcopallialis (FA) and is located laterally from the lateral striatum (LSt) in the ventrolateral telencephalon (Figures 2a, g and 3a, g). Through its course along the anterior–posterior axis, AA is further encompassed dorsomedially by the beginning of AD around the anterior–posterior coordinate A 7.80 (Figures 2a, 3a) and AI and is medially displaced by AI and ventrally by AV. AA showed very thin, fine fibers if compared to AD, AV, and AI (Figure 3a, b). AA-cells showed comparable cell sizes to AD. AD and AI can be easily delineated by their different cyto- and myelo-architecture (Figures 2b, c, h, i, 3a–l). AD is delineated from the nidopallium by the Lamina arcopallialis dorsalis (LAD; Figures 2b–d, 3b–e). Additionally, AD could be further subdivided into the intra-nuclear structures lateral arcopallium dorsale (ADl) and medial arcopallium dorsale (ADm) based on different myeloarchitectures (Figure 3b–l). Particularly, crossing fibers from the tractus dorsoarcopallialis (DA) demarcated ADl. The cyto- and myeloarchitecture of AI differed conspicuously from the surrounding regions. AI cells showed relatively large cell bodies compared to the other arcopallial regions (Figures 4–6). Further, many thick fibers that join the tractus occipitomesencephalicus (OM) characterized AI (Figure 3b–f, h–l). The finer and thinner fibers seen at the more posterior levels of AI belong to the tractus occipitomesencephalicus, pars hypothalami (HOM; Figure 3f, l). Additionally, a dorsal and a ventral part of AI (AId and AIv) were noticed. AId mostly corresponds to Aidv while AIv corresponds to Ai as defined in Kröner and Güntürkün (1999). Both substructures differ in their cellular- and myelo-architecture, with thinner fibers in AId compared to AIv (Figure 3b–f, h–l). As described earlier, AV showed differences in the cellular architecture and connectivity compared to the surrounding regions AI, AM, and PoAb (Zeier & Karten, 1971, Kröner & Güntürkün, 1999; Atoji et al., 2006; Shanahan et al., 2013, Letzner, Simon, & Güntürkün, 2016). Particularly, the cross sections of thick fibers that travel along the anterior posterior axis around atlas level 6.75 and pass across AV at more anterior levels characterized the shape of AV. Around atlas levels 7.50–7.25 an intra-nuclear substructure was detectable, which we named the medial part of the arcopallium ventral (AVm). AVm showed larger cell bodies compared to AV (Figure 4a–c) and thick fiber bundles that join OM (Figure 3b, c, h–i). According to Atoji and colleagues (2006, 2009), AM was subdivided into a medially located cell-dense, dark stained division with large cells (AMm) and a less cell-dense, parvocellular division (AMp) located laterally (Figures 2c–f, i–l, 5g, h, 6d). AMp was further characterized by a many thick fibers that travel through AM in the median axis (Figure 3d–f, j–l). The most caudal part of the arcopallium is a small, crescent-shaped subregion of the arcopallium that begins around atlas level 5.25 and is located between the amygdala nuclei PoAc and PoAb (Figures

TABLE 3 Significant differences between receptor densities in the main subregions of the arcopallium/amygdala complex

Subregion	AA	AD	AM	AI	AV	AP	PoAb	PoAc	TnA	SpA	NCVl
AA		M_2**	AMPA** Kainate** $GABA_A$* M_1**	M_2**	AMPA** M_1** M_2** $\alpha_4\beta_2$** α_2**	AMPA* Kainate** $GABA_A$* M_1** $\alpha_4\beta_2$*	$GABA_A$* M_2** $\alpha_4\beta_2$**	AMPA* Kainate** M_1** $\alpha_4\beta_2$** α_1**	Kainate** $GABA_A$** M_1** $\alpha_4\beta_2$** α_2** $D_{1/5}$**	NMDA** M_1** M_2** $\alpha_4\beta_2$** α_2**	AMPA* Kainate* M_1** M_2** α_1**
AD	M_2**		Kainate** $GABA_A$** M_1** M_2** $\alpha_4\beta_2$** 5-HT_{1A}**	NMDA* $GABA_A$** M_1** M_2* α_1** α_2* 5-HT_{1A}**	Kainate** NMDA** $GABA_A$** M_1** M_2** $\alpha_4\beta_2$** α_1** α_2** 5-HT_{1A}** $D_{1/5}$**	$GABA_A$** M_1** M_2* $\alpha_4\beta_2$* 5-HT_{1A}**	AMPA* $GABA_A$** M_1** M_2** α_1** 5-HT_{1A}* $D_{1/5}$**	NMDA** M_1** M_2** $\alpha_4\beta_2$** α_1** $D_{1/5}$*	Kainate** NMDA** $GABA_A$** M_1** M_2** $\alpha_4\beta_2$** α_1** α_2** 5-HT_{1A}** $D_{1/5}$**	AMPA** Kainate** NMDA** M_1** $\alpha_4\beta_2$** α_2** 5-HT_{1A}** $D_{1/5}$**	NMDA** M_1** M_2** α_1** $D_{1/5}$*
AM	AMPA** Kainate** $GABA_A$* M_1**	Kainate** $GABA_A$** M_1** M_2** $\alpha_4\beta_2$** 5-HT_{1A}**		Kainate** NMDA** $GABA_A$** M_1** M_2** $\alpha_4\beta_2$** α_1* α_2** 5-HT_{1A}**	Kainate** NMDA** $GABA_A$** M_1* M_2** $\alpha_4\beta_2$** α_1** α_2** 5-HT_{1A}**	5-HT_{1A}*	AMPA** $GABA_A$** M_2** $D_{1/5}$*	NMDA* $GABA_A$** M_1** M_2* $\alpha_4\beta_2$** α_1** 5-HT_{1A}** $D_{1/5}$**	Kainate* NMDA** $GABA_A$** M_1** $\alpha_4\beta_2$** α_1* α_2** $D_{1/5}$*	AMPA* Kainate** NMDA** M_2** $\alpha_4\beta_2$* α_2** 5-HT_{1A}*	NMDA* $GABA_A$** α_1** $D_{1/5}$**
AI	M_2**	NMDA* $GABA_A$** M_1** M_2* α_1** α_2* 5-HT_{1A}**	Kainate** NMDA** $GABA_A$** M_1** M_2** $\alpha_4\beta_2$** α_1* α_2** 5-HT_{1A}**		AMPA** Kainate** NMDA** M_1** M_2** $\alpha_4\beta_2$** α_2** 5-HT_{1A}**	Kainate** NMDA** $GABA_A$** M_1** M_2* α_2* 5-HT_{1A}**	AMPA* Kainate** $GABA_A$** M_1* M_2** $\alpha_4\beta_2$* 5-HT_{1A}** $D_{1/5}$**	NMDA** M_1** M_2** $\alpha_4\beta_2$** α_1** α_2** $D_{1/5}$**	Kainate** $GABA_A$** M_1** M_2* $\alpha_4\beta_2$** α_2** 5-HT_{1A}** $D_{1/5}$*	AMPA** Kainate** NMDA** M_1** $\alpha_4\beta_2$** α_2** 5-HT_{1A}**	Kainate* NMDA** M_1** M_2** α_1**
AV	AMPA** M_1** M_2** $\alpha_4\beta_2$** α_2**	Kainate** NMDA** $GABA_A$** M_1** M_2** $\alpha_4\beta_2$** α_1** α_2** 5-HT_{1A}** $D_{1/5}$**	Kainate** NMDA** $GABA_A$** M_1* M_2** $\alpha_4\beta_2$** α_1** α_2** 5-HT_{1A}**	AMPA** Kainate** NMDA** M_1** M_2** $\alpha_4\beta_2$** α_2** 5-HT_{1A}**		Kainate** $GABA_A$** α_2** 5-HT_{1A}** $D_{1/5}$*	AMPA** Kainate** NMDA** $GABA_A$** M_2** $\alpha_4\beta_2$* α_2** 5-HT_{1A}**	Kainate** M_1** $\alpha_4\beta_2$* α_1** α_2** $D_{1/5}$**	AMPA* Kainate** NMDA** $GABA_A$** M_1** M_2** $\alpha_4\beta_2$** α_2** 5-HT_{1A}**	AMPA** Kainate* NMDA** M_2** α_2** 5-HT_{1A}**	Kainate** α_1** α_2** $D_{1/5}$**
AP	AMPA* Kainate** $GABA_A$* M_1** $\alpha_4\beta_2$*	$GABA_A$** M_1** M_2* $\alpha_4\beta_2$* 5-HT_{1A}**	5-HT_{1A}*	Kainate** NMDA** $GABA_A$** M_1** M_2* α_2* 5-HT_{1A}**	Kainate** NMDA** $GABA_A$** α_2** 5-HT_{1A}** $D_{1/5}$*		AMPA** M_2* α_2** $D_{1/5}$*	Kainate* NMDA** $GABA_A$** M_1** α_1** 5-HT_{1A}**	AMPA** NMDA** $D_{1/5}$*	AMPA** Kainate** NMDA** $GABA_A$* $D_{1/5}$*	NMDA** $GABA_A$** α_1** 5-HT_{1A}*
PoAb	$GABA_A$* M_2** $\alpha_4\beta_2$**	AMPA* $GABA_A$** M_1** M_2** α_1** 5-HT_{1A}* $D_{1/5}$**	AMPA** $GABA_A$** M_2** $D_{1/5}$*	AMPA* Kainate** $GABA_A$** M_1* M_2** $\alpha_4\beta_2$* 5-HT_{1A}** $D_{1/5}$**	AMPA** Kainate** NMDA** $GABA_A$** M_2** $\alpha_4\beta_2$* α_2** 5-HT_{1A}**	AMPA** M_2* α_2** $D_{1/5}$*		AMPA** NMDA* $GABA_A$** M_2* $\alpha_4\beta_2$** α_1** 5-HT_{1A}** $D_{1/5}$**	Kainate** M_2** $\alpha_4\beta_2$** α_2**	Kainate** NMDA* $GABA_A$** M_2** α_2**	AMPA* $GABA_A$** M_2* α_1** 5-HT_{1A}** $D_{1/5}$**

(Continues)

TABLE 3 (Continued)

Subregion	AA	AD	AM	AI	AV	AP	PoAb	PoAc	TnA	SpA	NCVl
PoAc	AMPA* Kainate** M_1** $\alpha_4\beta_2$** α_1**	NMDA** M_1** M_2** $\alpha_4\beta_2$** α_1** $D_{1/5}$*	NMDA* $GABA_A$** M_2* $\alpha_4\beta_2$** α_1** 5-HT_{1A}** $D_{1/5}$**	M_1** M_2** $\alpha_4\beta_2$** α_1** α_2** $D_{1/5}$**	Kainate** M_1** $\alpha_4\beta_2$* α_1** α_2** $D_{1/5}$**	Kainate* NMDA** $GABA_A$** M_1** α_1** 5-HT_{1A}**	AMPA** NMDA* $GABA_A$** M_2* $\alpha_4\beta_2$** α_1** 5-HT_{1A}** $D_{1/5}$**		Kainate** NMDA** $GABA_A$** M_1** α_1** α_2** 5-HT_{1A}** $D_{1/5}$**	AMPA* Kainate** NMDA** M_2** $\alpha_4\beta_2$** α_1** α_2** 5-HT_{1A}** $D_{1/5}$**	Kainate* M_1** $\alpha_4\beta_2$* 5-HT_{1A}**
TnA	Kainate** $GABA_A$** M_1** $\alpha_4\beta_2$** α_2** $D_{1/5}$**	Kainate** NMDA** $GABA_A$** M_1** M_2** $\alpha_4\beta_2$** α_1** α_2** 5-HT_{1A}** $D_{1/5}$**	Kainate* NMDA** $GABA_A$** M_1** $\alpha_4\beta_2$** α_1* α_2** $D_{1/5}$*	Kainate** $GABA_A$** M_1** M_2* $\alpha_4\beta_2$** α_2** 5-HT_{1A}** $D_{1/5}$*	AMPA* Kainate** NMDA** $GABA_A$** M_1** M_2** $\alpha_4\beta_2$** α_2** 5-HT_{1A}**	AMPA** NMDA** $D_{1/5}$*	Kainate** M_2** $\alpha_4\beta_2$** α_2**	Kainate** NMDA** $GABA_A$** M_1** α_1** α_2** 5-HT_{1A}** $D_{1/5}$**		Kainate** NMDA** $GABA_A$** M_1** M_2* $\alpha_4\beta_2$* α_2**	NMDA** $GABA_A$** $\alpha_4\beta_2$** α_1** α_2** 5-HT_{1A}** $D_{1/5}$**
SpA	NMDA** M_1** M_2** $\alpha_4\beta_2$** α_2**	AMPA** Kainate** NMDA** M_1** $\alpha_4\beta_2$** α_2** 5-HT_{1A}** $D_{1/5}$**	AMPA* Kainate** NMDA** M_2** $\alpha_4\beta_2$* α_2** 5-HT_{1A}*	AMPA** Kainate** NMDA** M_1** $\alpha_4\beta_2$** α_2** 5-HT_{1A}**	AMPA** Kainate* NMDA** M_2** α_2** 5-HT_{1A}**	AMPA** Kainate** NMDA** $GABA_A$* $D_{1/5}$*	NMDA* $GABA_A$** M_2** α_2**	AMPA* Kainate** NMDA** M_2** $\alpha_4\beta_2$** α_1** α_2** 5-HT_{1A}** $D_{1/5}$**	Kainate** NMDA** $GABA_A$** M_1** M_2* $\alpha_4\beta_2$* α_2**		Kainate** NMDA** M_2** α_1** α_2** 5-HT_{1A}** $D_{1/5}$**
NCVl	AMPA* Kainate* M_1** M_2** α_1**	NMDA** M_1** M_2** α_1** $D_{1/5}$*	NMDA* $GABA_A$** α_1** $D_{1/5}$**	Kainate* NMDA** M_1** M_2** α_1**	Kainate** α_1** α_2** $D_{1/5}$**	NMDA** $GABA_A$** α_1** 5-HT_{1A}*	AMPA* $GABA_A$** M_2* α_1** 5-HT_{1A}** $D_{1/5}$**	Kainate* M_1** $\alpha_4\beta_2$* 5-HT_{1A}**	NMDA** $GABA_A$** $\alpha_4\beta_2$** α_1** α_2** 5-HT_{1A}** $D_{1/5}$**	Kainate** NMDA** M_2** α_1** α_2** 5-HT_{1A}** $D_{1/5}$**	

Each receptor type was tested separately with pair-wise Wilcoxon-rank test if the Friedman ANOVA showed regional differences between subregions. **$T = 0$; $p < .05$, * $T = 1$; $p < .05$.

2e, f, k, l, 6). It was also described in Atoji et al. (2006) as the posterior part of AI. AP has a different connectivity from PoAc and PoAb (Atoji et al., 2006) and showed cells with larger cell bodies if compared to PoAc. Cells in PoAb also showed large cell bodies, but cells were less dense and patchier distributed compared to AP (Figure 6e, f). AP and AI differed considerably in their myelo-architecture. AP showed intra nuclear thin fiber labeling and no larger crossing fibers like AI.

The amygdala nuclei were subdivided into the area subpallialis amygdalae (SpA), which is a subpallial part of the extended amygdala in birds (Yamamoto et al., 2005), the nucleus taeniae amgygdalae (TnA; Reiner et al., 2004) and according to Atoji and colleagues (2006) in a basal and a compact division of the nucleus posterioris amygdalopallii (PoAb and PoAc). Further, we included the bed nucleus of the stria terminals pars lateralis (BSTL), that was defined based on its cytoarchitectonic characteristics that have been described in detail earlier (Atoji et al., 2006). The borders of TnA were nicely resolved with the cell staining and TnA could be distinguished from the surrounding areas by its small-sized cells (Figures 2c, 5b). The myelin staining showed thin fibers in TnA and a few thick fibers but with a smaller diameter compared to AI and AM that travel along the anterior–posterior axis of TnA at the border to AM (fascicles from OM; Figure 3d, e). Both, PoAc and PoAb differed considerably in their cyto- and myelo-architecture (Figures 2d–f, 3d–f). While PoAc showed a compact mass of small cells, PoAb is speckled with cells with larger cell bodies (Figures 6c, e). Further, PoAb is characterized by thin and short fibers that were often transversally directed, while in PoAc many longitudinal fibers were detected.

3.2 | Quantitative analysis of the receptor-binding site densities in the arcopallium/amygdala complex

Quantitative receptor data of the arcopallium/amygdala complex is presented in form of color-coded autoradiographs for each receptor at different atlas levels of a series of five cross sections with a gap of approximately 500 μm between each slice to highlight the regional differences in receptor expression that nicely resolve distinct subregions and intra-nuclear substructures (Figures 7–10). Additionally, binding site densities of all receptors ± *SEM* are presented in a 2-dimensional polar coordinate-plot to construct a multi-receptor fingerprint for each

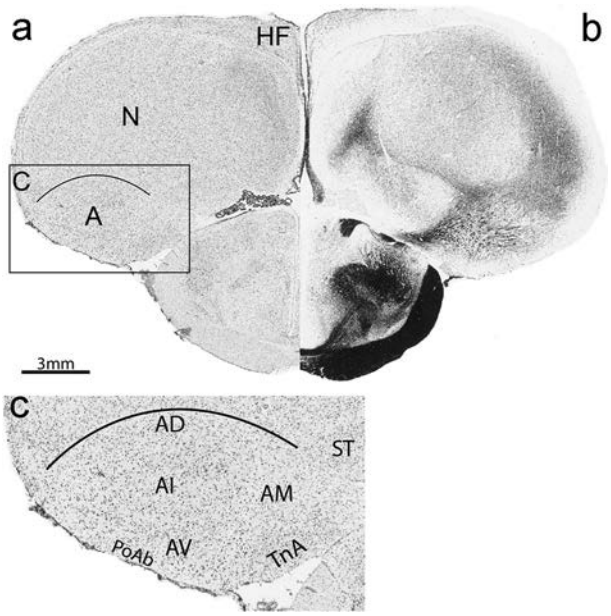

FIGURE 1 Nissl and myelin stained coronal section of the forebrain of the pigeon. (a) Nissl stained and (b) myelin stained coronal section at atlas level A 6.75 (Karten & Hodos, 1967). The boxed area indicates the region of interest: the arcopallium/amygdala complex. Scale bar 3 mm. (c) Enlarged image of the arcopallium/amygdala complex labeled in (a). A, arcopallium; AD, arcopallium dorsale; AI, arcopallium intermedium; AM, arcopallium mediale; AV, arcopallium ventrale; HF, hippocampal formation; N, nidopallium; PoAb, Nucleus posterioris amygdalopallii pars basalis; ST, striatum; TnA, Nucleus taeniae amygdalae

analyzed subregion (Figure 11a–l). We also present the receptor data for the adjacent areas of the arcopallium/amygdala complex, the posterior lateral striatum (LSt, from atlas level A 6.75–6.25; Figure 11c) and the lateral division of the nidopallium caudoventrale (NCVl); Figure 11i). Data for the intra-nuclear substructures is provided separately in histograms (Figure 12a–k). Detailed numbers of receptor densities and statistics are summarized in Tables 2 and 3. In the following subsections, we describe the highlights in receptor densities that resolved the different subregions and intra-nuclear structures one by one.

AA The anterior tip of the arcopallium is high in AMPA, kainate and $GABA_A$ receptor densities (Table 2). In contrast to the surrounding regions AD and AI, AA expressed lower M_2-receptor densities and a trend towards higher kainate receptor densities was detected. If compared to AV, higher M_1, M_2 and α_2-receptor and lower AMPA and nACh ($\alpha_4\beta_2$ subtype) receptor levels were found (Tables 2 & 3). The overall receptor expression was comparable to AD and AI (Figures 11 a, d, e; Tables 2, 3).

AD Receptor densities in AD differed from the dorsally located PoAc for NMDA, M_1, M_2, nACh ($\alpha_4\beta_2$ subtype), α_1- and $D_{1/5}$ receptors (Figures 7–10; Table 3). Additionally, AD had conspicuously high M_1 and M_2 receptor densities if compared to the other arcopallial regions (Figure 8; Table 2) and α_2-receptor expression rendered distinctively the crescent structure of AD (Figure 9). Except AMPA receptors, all measured receptors were differentially expressed in AD compared to AV (Figures 7–10; Tables 2, 3). The fingerprints of AD and AI appeared very similar (Figure 11d, e). ADl and ADm differed in kainate, NMDA, $GABA_A$, and 5-HT_{1A} receptors (Figure 12b–d, j). This delineation was primarily observed with the heterogeneously distribution of kainate receptors in ADl and ADm (Figure 7).

AI AI showed higher densities of M_2 receptors and lower densities of kainate receptors compared to the ventral region of the arcopallium (Figures 7, 8; Tables 2, 3). $GABA_A$ receptor expression was higher in AI compared to AM, AD, and AP and nicely resolved the borders to these neighboring regions (Figure 8). Further, the borders of the intermediate arcopallial region were covered with a higher 5-HT_{1A}-receptor density compared to the surrounding regions (Figure 10). The sub differentiation of AI into AId and AIv was supported by six significant differences in receptor binding sites (Figure 12c–f, i, j) and highlighted by a higher M_1-, M_2- α_2-, and 5-HT_{1A}-receptor expression in AId (Figures 8–10).

AV A high kainate receptor density delineates the ventral arcopallium from the dorsally located regions AI and AD and the medially located regions AM and TnA (Figure 7). AV additionally showed higher AMPA receptor densities if compared to AA, AI, TnA, SpA, and PoAb, and higher NMDA receptor densities if compared to AD, AI, AM, AP, PoAb, TnA, and SpA (Figure 7; Tables 2, 3). Further, a high $GABA_A$ receptor expression and relatively low M_2 receptor densities compared to the other arcopallial regions characterized AV (Figure 8; Tables 2, 3). AVm differed in kainate-, NMDA-, $GABA_A$-, M_1-, α_2-, 5-HT_{1A}-, and $D_{1/5}$- receptor densities from AV and AVm showed particularly lower $GABA_A$ receptor amounts if compared to AV (Figures 8, 12b–e, i–k).

AM Kainate and $GABA_A$ receptors showed relatively low levels in the medial arcopallium if compared to the other arcopallial regions, except AP (Figures 7, 8). AMPA receptor expression in AM was comparable to AD, AV and AP, and higher compared to AA and AI and the ventrally located TnA (Figure 7; Tables 2, 3). The receptor architecture of AM was different if compared to the other arcopallial regions AI and AV (Tables 2, 3) that is also visualized in the receptor fingerprint (Figure 11d, e, g). The substructures AMm and AMp were nicely resolved by the heterogeneously distribution of NMDA and 5-HT_{1A} receptors in AM (Figures 7, 10) and receptor densities differed in 8 out of the 11 measured types (Figure 12a–k).

AP AP differed from AI by its higher amounts of NMDA, α_2 and lower amounts of kainate, $GABA_A$, M_1, M_2, and 5-HT_{1A} receptors (Figures 7–11e, l; Tables 2, 3). Particularly, the glutamatergic receptors demarcated PoAc, AP and PoAb (Figure 7; Tables 2, 3), and α_2 receptors showed intense labeling of AP compared to PoAc (Figure 9; Tables 2, 3). AP showed only a significant difference in 5-HT_{1A} receptor expressions compared to AM, but further comparisons between both regions indicated differences by a trend for NMDA, $\alpha_4\beta_2$ and α_2 receptor densities. The overall receptor architecture of AP is highly similar to AM (Figure 11g, l).

PoA High densities of kainate, α_1, 5-HT_{1A} or $D_{1/5}$ receptors highlighted PoAc if compared to the surrounding structures AD, AP and NCVl (Figures 7, 9, 10; Tables 2, 3), whereas PoAb was separated from AV by lower AMPA, kainate, NMDA, $GABA_A$, M_2, nACh ($\alpha_4\beta_2$ subtype) and 5-HT_{1A} receptor densities (Figures 7–10; Tables 2, 3). PoAc and PoAb differed significantly from each other in AMPA, NMDA, $GABA_A$, M_2, nACh ($\alpha_4\beta_2$ subtype), α_1, 5-HT_{1A} and $D_{1/5}$ receptor densities (Figure 12a, c–d, f–h, j–k; Tables 2, 3).

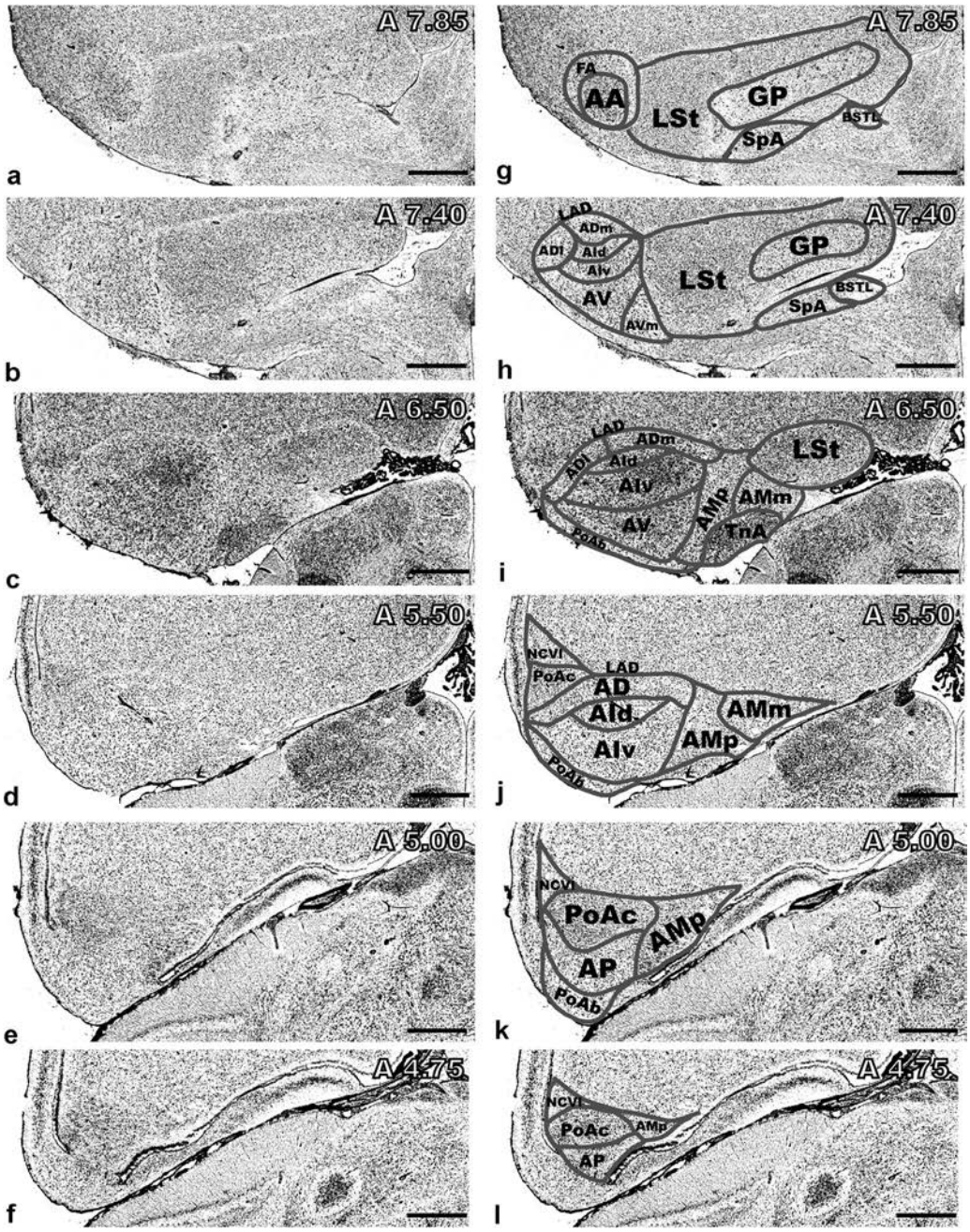

FIGURE 2 Representative Nissl stained coronal sections through the pigeon arcopallium/amygdala complex showing subregion boundaries at different rostro-caudal levels. (a–f) Nissl stained coronal sections of the arcopallium/amygdala complex. (g–l) Nissl stained coronal sections of the arcopallium/amygdala complex with the boundaries defined by (Atoji et al., 2006; Atoji & Wild, 2009; Karten & Hodos, 1967; Kröner & Güntürkün, 1999; Reiner et al., 2004; Shanahan et al., 2013; Yamamoto & Reiner, 2005; Zeier & Karten, 1971) and our own observations. These boundaries were defined solely based on cytoarchitectonical criteria and were used to identify regions of interest in receptor autoradiographs. The arcopallium/amygdala complex and the extended amygdala of pigeons comprises the following regions: AA, arcopallium anterius; AD, arcopallium dorsale; ADm, arcopallium dorsale pars medialis; ADl, arcopallium dorsale pars lateralis; AI, arcopallium intermedium; AId, arcopallium intermedium pars dorsalis; AIv, arcopallium intermedium pars verntralis; AM, arcopallium mediale; AMp, arcopallium mediale pars parvocellularis; AMm, arcopallium mediale pars magnocellularis; AP, arcopallium posterioris; AV, arcopallium ventrale; AVm, arcopallium ventrale pars medialis; BSTL, Bed nucleus of the Stria Terminalis, pars lateralis; PoAb, nucleus posterioris amygdalopalii pars basalis; PoAc, nucleus posterioris amygdalopalii pars compacta; SpA, area subpallialis amygdalae; TnA, nucleus taeniae amygdalae. Scale bar 1200 μm in (a), 1000 μm in (b), 1160 μm in (c), 1125 μm in (d), 1150 μm in (e), 1125 μm in (f), 1200 μm in (g), 1000 μm in (h), 1160 μm in (i), 1125 μm in (j), 1150 μm in (k), 1125 μm in (l)

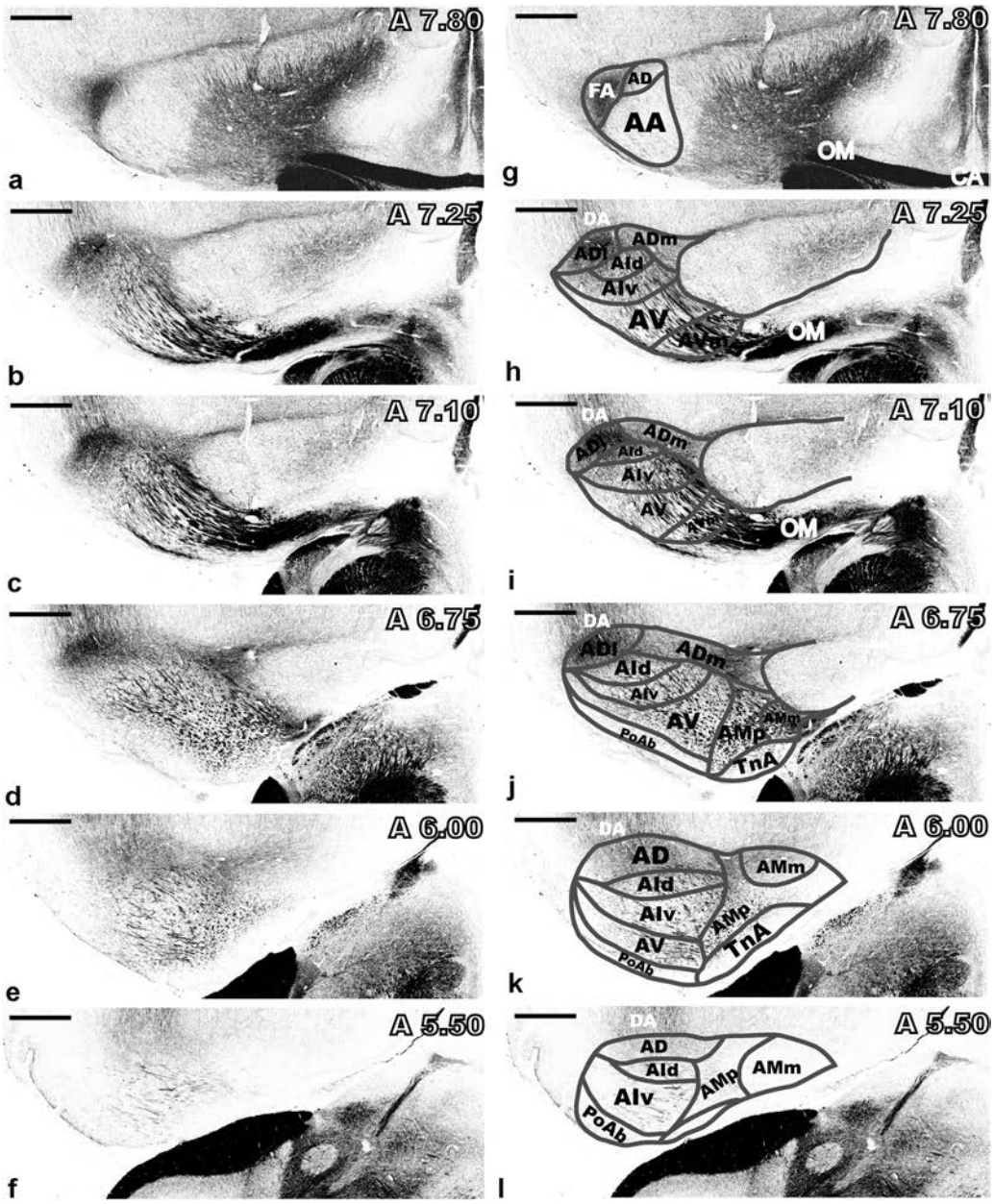

FIGURE 3 Representative myelin stained coronal sections of the pigeon arcopallium/amygdala complex showing subregion boundaries at different rostro-caudal levels. (a–f) Myelin-stained coronal sections of the arcopallium/amygdala complex. (g–l) Myelin-stained coronal sections of the arcopallium/amygdala complex with boundaries and labels. Differences in fiber architecture in the arcopallial subregions and their intra-nuclear substructures were of particular help for the delineation of structures in receptor autoradiographs and defining boundaries between ADl and ADm. For abbreviations see legend of Figure 2. Scale bar 1300 μm in (a), 1190 μm in (b), 1400 μm in (c), 1300 μm in (d), 1300 μm in (e), 1250 μm in (f), 1300 μm in (g), 1190 μm in (h), 1400 μm in (i), 1300 μm in (j), 1300 μm in (k), 1250 μm in (l)

TnA High M_2, nACh ($\alpha_4\beta_2$ subtype) and α_2 receptor densities characterized this subdivision of the arcopallium/amgygdala complex (Figures 8, 9). TnA further differed from the neighboring AM by eight receptors and showed a substantial peak in α_2 receptor density (Figures 9, 11l; Tables 2, 3). The majority of similarities in the overall receptor architecture were detected between TnA and AP (Table 3) and visualized in Figure 11h, l.

SpA This area, which is a subpallial part of the extended amygdala in birds, expressed 2.6-fold lower amounts of $GABA_A$ receptors compared to LSt that nicely resolved the border between those areas (Figure 8). SpA further showed higher densities of kainate, M_2, nACh ($\alpha_4\beta_2$ subtype) and α_2 receptors and lower AMPA, NMDA, and 5-HT_{1A} receptors if compared to the neighboring subregion AM (Tables 2, 3). If compared to the other analyzed regions, the receptor fingerprint of SpA appeared differentially (Figure 12b).

In some slices, we also managed to analyze the bed nucleus of the stria terminals pars lateralis (BSTL), which is considered to be a part of the extended amygdala of birds. However, we could not sample a sufficient receptor data set to quantify it.

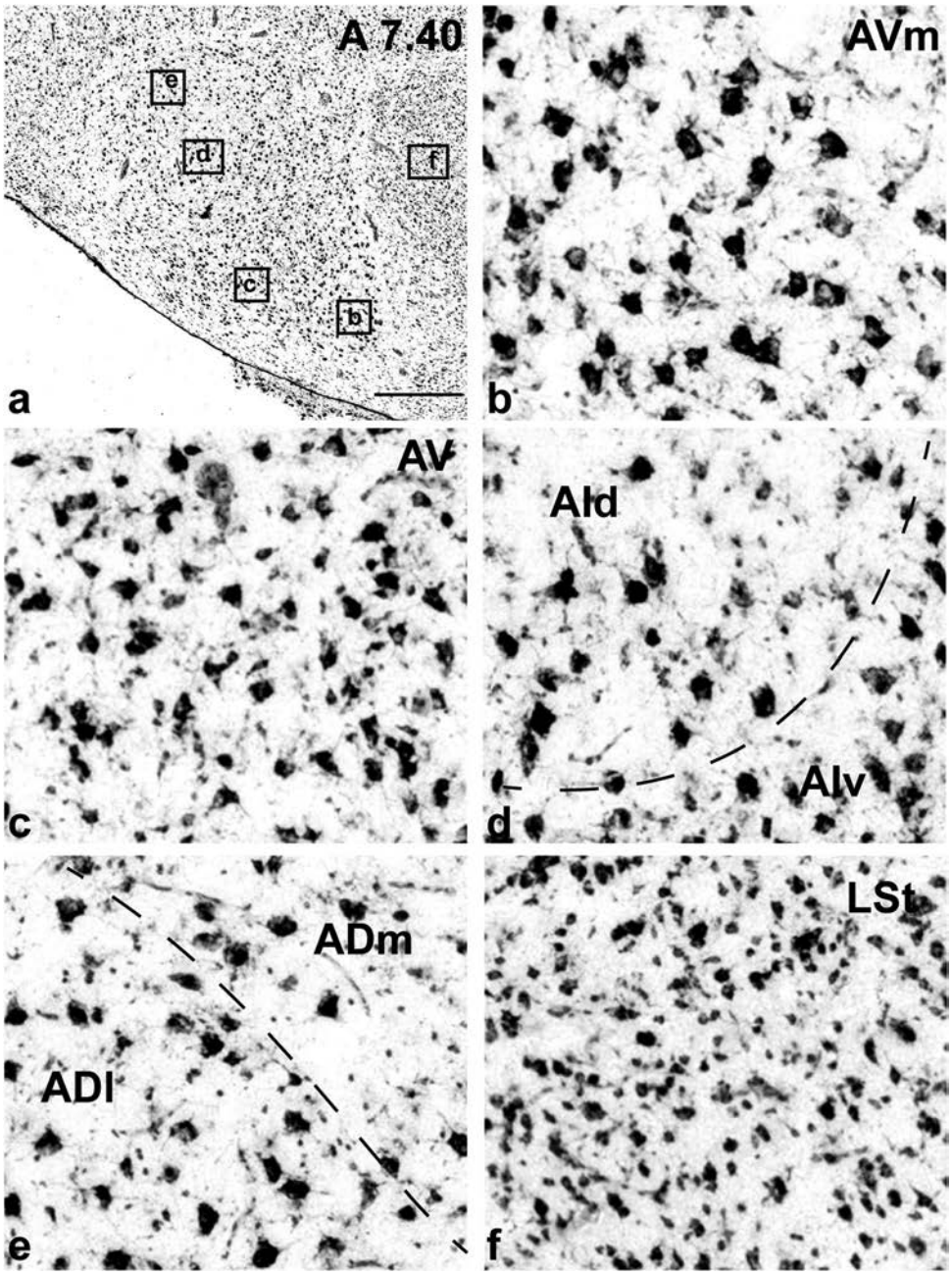

FIGURE 4 Enlarged image of the arcopallium at atlas level A 7.40 (a) and details of the cellular architecture (b–f). (b–f) Enlargement of boxes labeled in a (6× magnification) showing the cellular densities and cell sizes in the different subregions of the arcopallium. Scale bar 600 μm

The resulting new atlas from the AP coordinate A 7.75–4.50 is based, therefore, on the overlay of cellular/fiber-architectonic and receptor-density information, and is presented in Figure 13.

3.3 | Combined analysis of the overall receptor architecture in the arcopallium/amygdala complex

Overall (dis)similarities in the neurotransmitter receptor architecture between subregions of the arcopallium/amygdala complex, NCVl and posterior LSt are shown in a cladogram of a hierarchical cluster analysis (Figure 14). The hierarchical cluster analysis provided two main clusters of the analyzed subdivisions that split further up in different branches (cophenetic correlation coefficient $c = 0.60$). One main cluster groups the seven regions NCVl, PoAc, TnA, AP, AV, PoAb and AM (Cluster I), and the other cluster comprises the five regions posterior LSt, SpA, AA, AI, and AD (Cluster II, Figure 14). Further, in Cluster I, NCVl and PoAc are separated from TnA, AP, AV, PoAb, and AM, and in Cluster II, LSt and SpA are separated from AA, AI, and AD. In Cluster I, the lowest Euclidian distance was observed between PoAb and AM, while in Cluster II, the lowest Euclidian distance was observed between AI and AD.

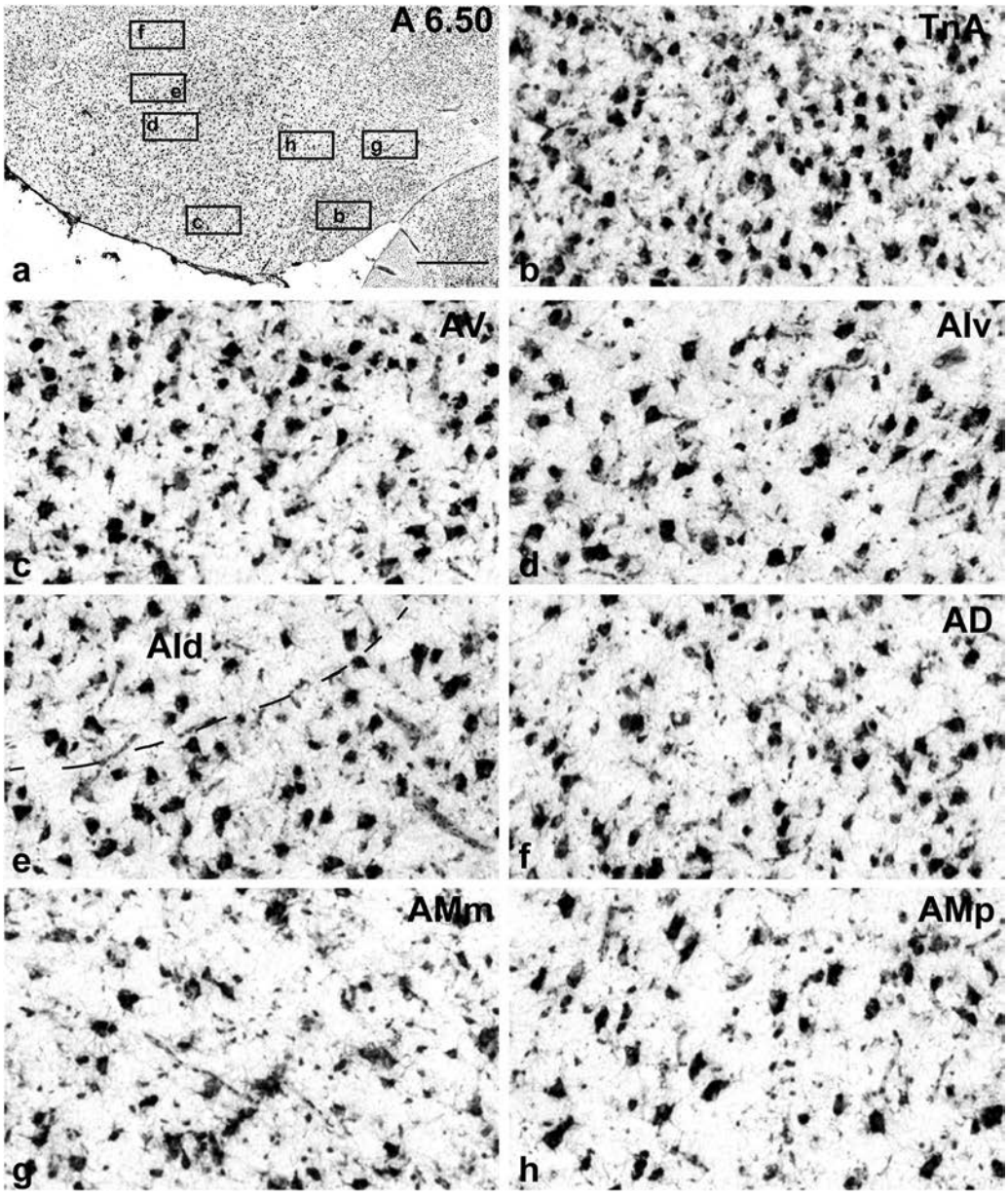

FIGURE 5 Enlarged image of the arcopallium/amygdala complex at atlas level A 6.50 (a) and details of the cellular architecture (b–h). (b–h) Enlargement of boxes labeled in a (8× magnification) showing the cellular densities and cell sizes in the different subregions of the arcopallium. Scale bar 700 μm

4 | DISCUSSION

The regionally different receptor densities mapped well onto several subregions of the arcopallium/amygdala complex in pigeons that have been in part previously described based on connectivity data and cellular analysis (Atoji et al., 2006; Karten & Hodos, 1967; Kröner & Güntürkün, 1999; Puelles, Martinez-de-la-Torre, Paxinos, Watson, & Martinez, 2007; Shanahan et al., 2013; Yamamoto et al., 2005). These subregions are: the arcopallium anterius (AA), the arcopallium ventrale (AV), the arcopallium dorsale (AD), the arcopallium intermedium (AI), the arcopallium mediale (AM), the arcopallium posterius (AP), the nucleus posterioris amygdalopallii pars basalis (PoAb) and pars compacta (PoAc), the nucleus taeniae amgygdalae (TnA) and the area subpallialis amygdalae (SpA). Based on our results, AV, AM, AD, and AI can be further subdivided into intra-nuclear substructures. Several important differences in receptor- cyto- and myelo-architecture highlighted the distinct subregions and intra-nuclear substructures that resulted into a new map of the pigeon arcopallium/amygdala complex. Together with data from previous studies, our results provide a high-resolution scheme of the pigeon's arcopallium/amygdala complex that can be used for future structural and functional studies. This will also improve the anatomic identification in different types of data sets from genetic approaches to functional studies in various avian species, may help to assess species-specific adaptations, and discover important basic neurochemical traits that may be conserved in the arcopallium/amygdala complex. Further, our data will facilitate the comparison

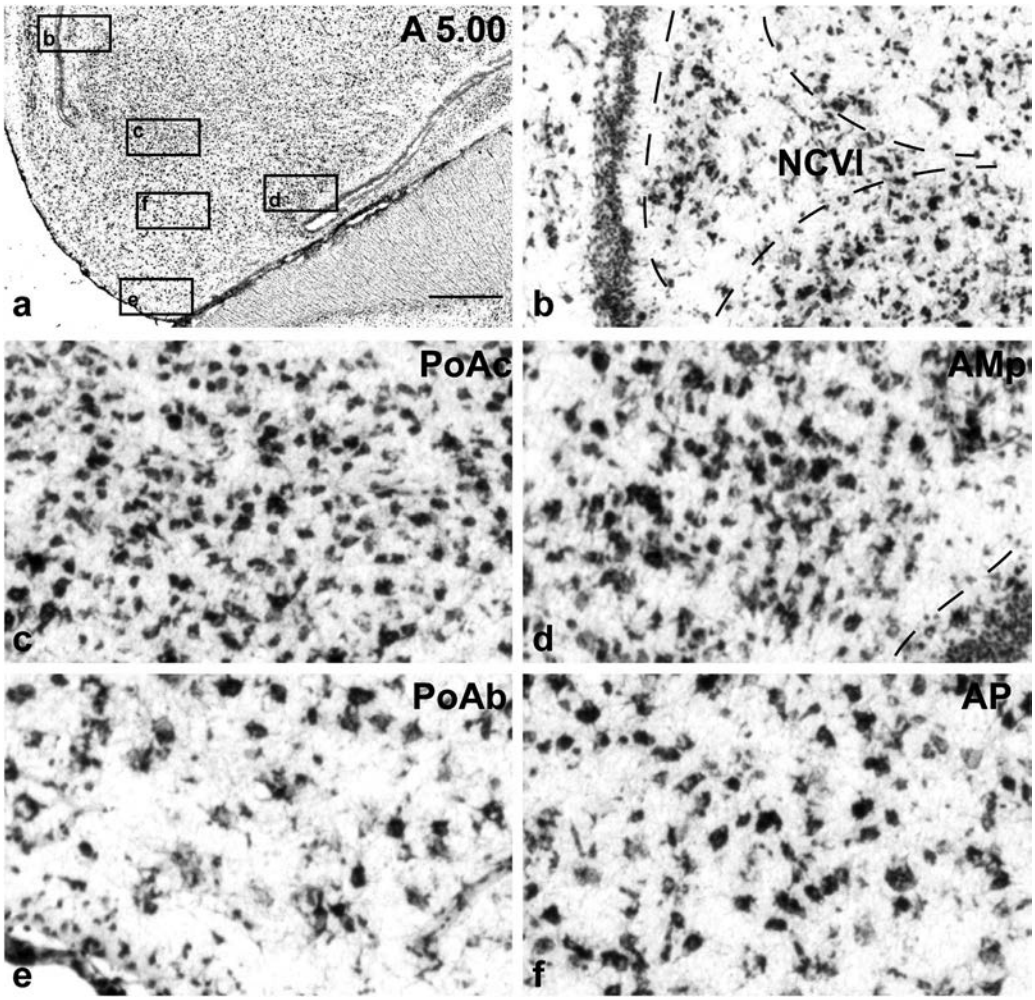

FIGURE 6 Enlarged image of the arcopallium/amygdala complex at atlas level A 5.00 (a) and details of the cellular architecture (b–f). (b–f) Enlargement of boxes labeled in a (8× magnification) showing the cellular densities and cell sizes in the different subregions of the arcopallium. Scale bar 600 μm

between the avian premotor and amygdala subregions with possibly corresponding homolog or homoplastic mammalian structures.

4.1 | The avian arcopallium/amygdala complex: previous studies and thoughts on homologies

According to the classic view of the 19th century, most of the avian telencephalon was supposed to be homologous to the mammalian basal ganglia (Edinger, 1896). This interpretation resulted in an avian brain nomenclature were Greek prefixes and the root word 'striatum' were combined to label the different substructures of the bird telencephalon (Ariens-Kappers, Huber, & Crosby, 1936; Edinger, 1903). Accordingly, the caudal ventrolateral portion of the telencephalon was termed archistriatum and suggested to be partly comparable to the mammalian amygdala. Much later and based on connectivity data, Zeier and Karten (1971) subdivided this area into four major regions: the archistriatum anterior, intermedium (with a dorsal portion), posterior (with a postero-ventral portion) and mediale. This delineation differs to some extent from the pigeon atlas of Karten and Hodos (1967). According to Zeier and Karten (1971) the posterior and medial archistriatum correspond to the amygdala since they are connected via the tractus occipitomesencephalicus, pars hypothalami (HOM) to the hypothalamus. In contrast, the archistriatum intermedium and anterior were supposed to be part of the sensorimotor system since they lack limbic projections and are connected via the tractus occipitomesencephalicus (OM) to various sensory and motor entities of thalamus and brainstem. According to Zeier and Karten (1971), only the anterior archistriatum received fibers both from the anterior commissure and from the tractus fronto-arcopallialis (FA), whereas the intermediate part received its input from the tractus arcopallialis dorsalis (DA). However, a new study revealed that the anterior commissure derives from both the anterior and the intermediate arcopallium (Letzner et al., 2016). Over the years, further subnuclei of the archistriatum were defined which will be discussed below.

At the beginning of the new millennium, neuroanatomists had reached the consensus that the view of the striatally dominated bird forebrain was outmoded and wrong. Accordingly, a revised nomenclature of the avian telencephalon was conceived (Reiner et al., 2004;

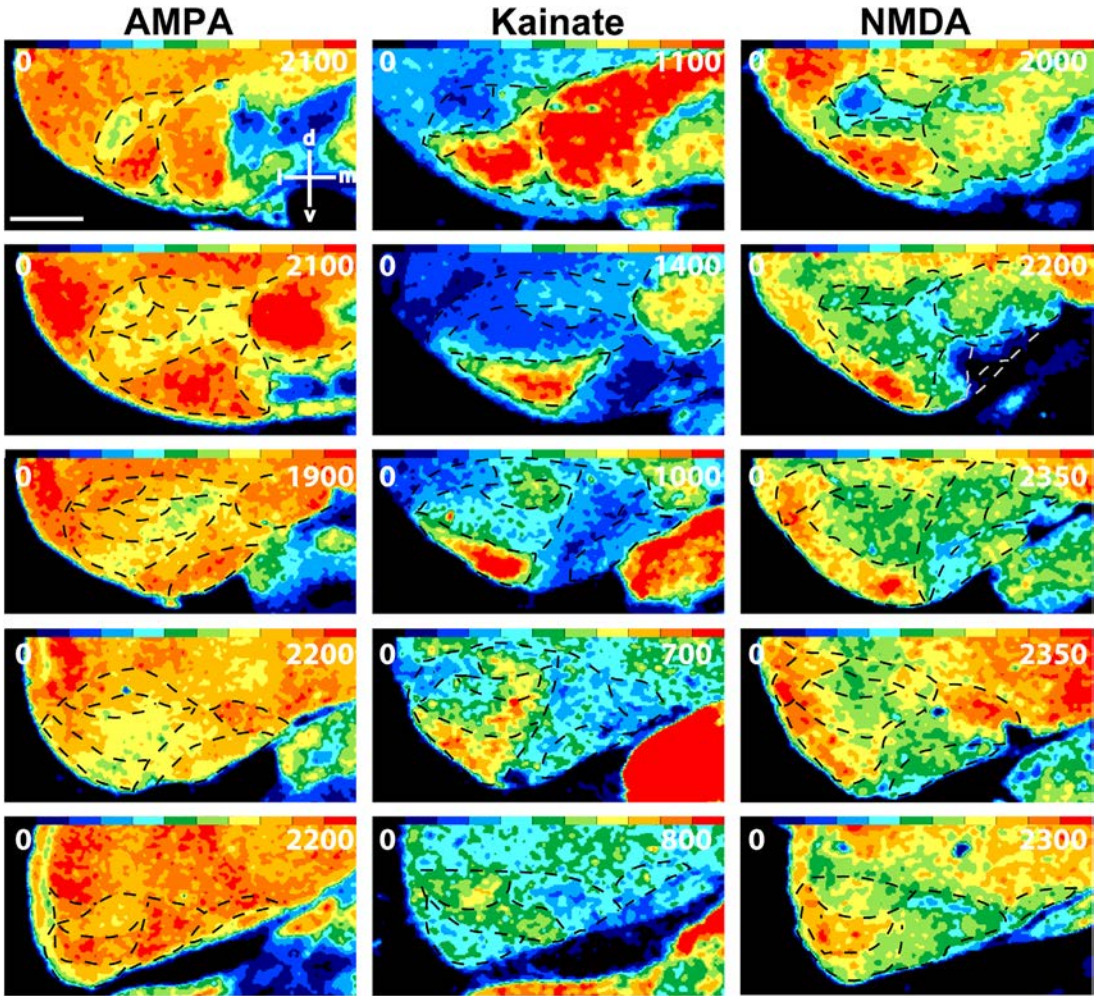

FIGURE 7 Color-coded autoradiographs showing the distribution and density of glutamate receptors at different rostro-caudal atlas levels of a series of five cross sections with a gap of approximately 500 μm between each slice of the arcopallium/amygdala complex. Left column: AMPA receptor expression in the arcopallium/amygdala complex from anterior (top) to posterior (down) levels. Middle column: Kainate receptor expression in the arcopallium/amygdala complex from anterior (top) to posterior (down) levels. Right column: NMDA receptor expression in the arcopallium/amygdala complex from anterior (top) to posterior (down) levels. Dashed lines show boundaries as depicted in Figures 2 and 3. Color scales code for the receptor densities in fmol/mg protein and are specific for each receptor type. Note that the red end of the scale bar indicates the best fit for the investigated arcopallium/amygdala substructures but not the maximum receptor density. Please use the atlas in Figure 13 to trace the labels of the different brain regions. Scale bar row 1–2: 1.8 mm, row 3–5: 3.5 mm [Color figure can be viewed at wileyonlinelibrary.com]

Jarvis et al., 2005) and along that line the archistriatum was subdivided into a premotor arcopallium complex and a limbic amygdala assembly of nuclei. Only the medial arcopallium was left undecided since it seemed to display both limbic and premotor features. Meanwhile further limbic associations of the medial arcopallium have been discovered and will be discussed further below (Atoji & Wild, 2009; Medina, Bupesh, & Abellán, 2011). In addition, some subnuclei of the arcopallial/amygdala complex can only be found in certain avian groups like those that learn their vocalizations (songbirds: robust nucleus of the arcopallium (RA); parrots: central nucleus of the anterior arcopallium (AAC); hummingbirds: vocal nucleus of the arcopallium (VA)).

To shed some light into the ongoing discussion of which subregions of the arcopallium/amygdala complex are limbic, Yamamoto and colleagues (2005a, 2005b) used different markers like the limbic associated membrane protein (LAMP) and the subpallial marker glutamate decarboxylase 65 (GAD65), to discover limbic and or subpallial components of the arcopallium/amygdala complex. This approach did not only show co-expression of these markers in TnA and SpA but also brought forward that the lateral and medial nuclei of the stria terminalis (BSTM and BSTL) of birds may be a part of the extended amygdala. Furthermore, these authors concluded that TnA should be subdivided into a lateral and medial pallial subnucleus. The weak labeling of the anterior two thirds of the arcopallium (including AA and AI) supported the suggestion of Zeier and Karten (1971) that these parts are of premotor nature. However, the dorsal arcopallium showed intense LAMP labeling which would be inconsistent with the former conclusion that this subregion is not limbic but is in line with other connectivity studies that showed inputs to AD from limbic regions like the piriform cortex, hippocampal formation, and TnA and outputs to the limbic medial and somatic lateral striatum (Atoji & Wild, 2006; Bingman, Casini, Nocjar, &

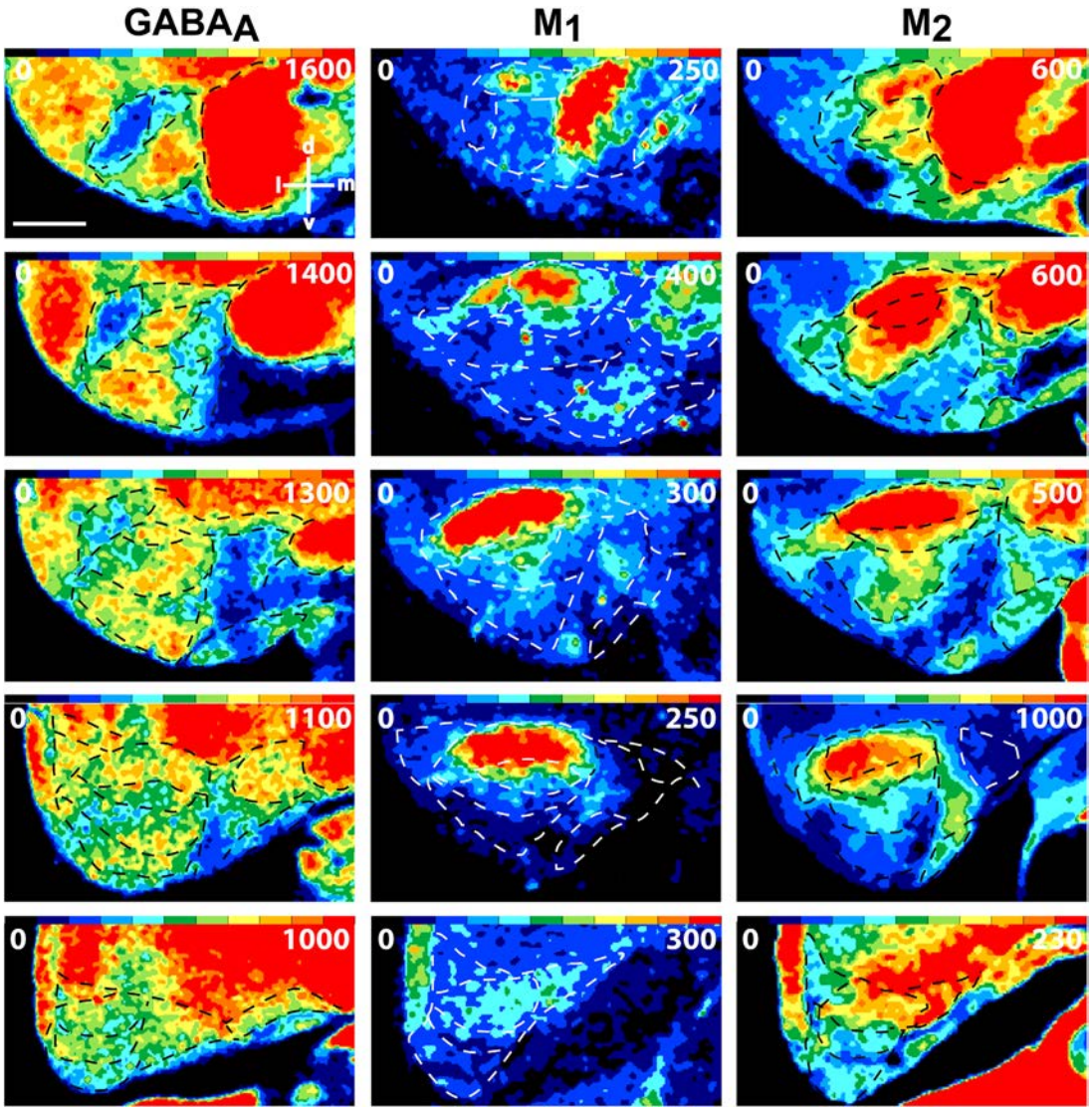

FIGURE 8 Color-coded autoradiographs showing the distribution and density of $GABA_A$ and muscarinergic cholinergic receptors at different rostro-caudal atlas levels of a series of five cross sections with a gap of approximately 500 μm between each slice of the arcopallium/amygdala complex. Left column: $GABA_A$ receptor expression in the arcopallium/amygdala complex from anterior (top) to posterior (down) levels. Middle column: M_1 receptor expression in the arcopallium/amygdala complex from anterior (top) to posterior (down) levels. Right column: M_2 receptor expression in the arcopallium/amygdala complex from anterior (top) to posterior (down) levels. Further explanations see Figure 7 [Color figure can be viewed at wileyonlinelibrary.com]

Jones, 1994; Veenman, Wild, & Reiner, 1995). Further, LAMP labeling showed that AD is distinct from AA (Yamamoto & Reiner, 2005). The posterior pallial amygdala (PoA) is also LAMP-rich, which is in line with its viscero-limbic connectivity (Zeier & Karten, 1971; Reiner et al., 2004). AM showed intense LAMP labeling as well, which would support the idea that AM is limbic (Zeier & Karten, 1971; Yamamoto & Reiner, 2005).

4.2 | The delineation of the arcopallium/amygdala complex based on receptor autoradiography, cyto- and myeloarchitecture

The cluster analysis of the overall receptor architecture of arcopallial, amygdala, striatal, and nidopallial subdivisions divided the investigated subdivisions into two main clusters with further subgroups that may be interpreted as either functionally or anatomically (dis)similar, possibly involved in different neuronal circuits. Herein, our results fit very well with the findings of a study that analyzed several pathway-tracing studies to construct a connectivity matrix ("structural connectome") for the telencephalon of the pigeon (Shanahan et al., 2013). In Cluster I, one group comprises PoAc and NCVl, both pallial subdivisions, adjacent regions and involved in viscero-limbic functions (Shanahan et al., 2013), and the second group comprises TnA, AP, AV, PoAb, and AM, which challenges the question if TnA is a subpallial part of the amygdala because all other regions of this cluster are of pallial origin. Further, the second group of Cluster I also splits up in more subgroups, one subgroup comprises TnA and AP, and the other AV, PoAb, and AM, with AV more distinct from AM/PoAb that is consistent with the finding

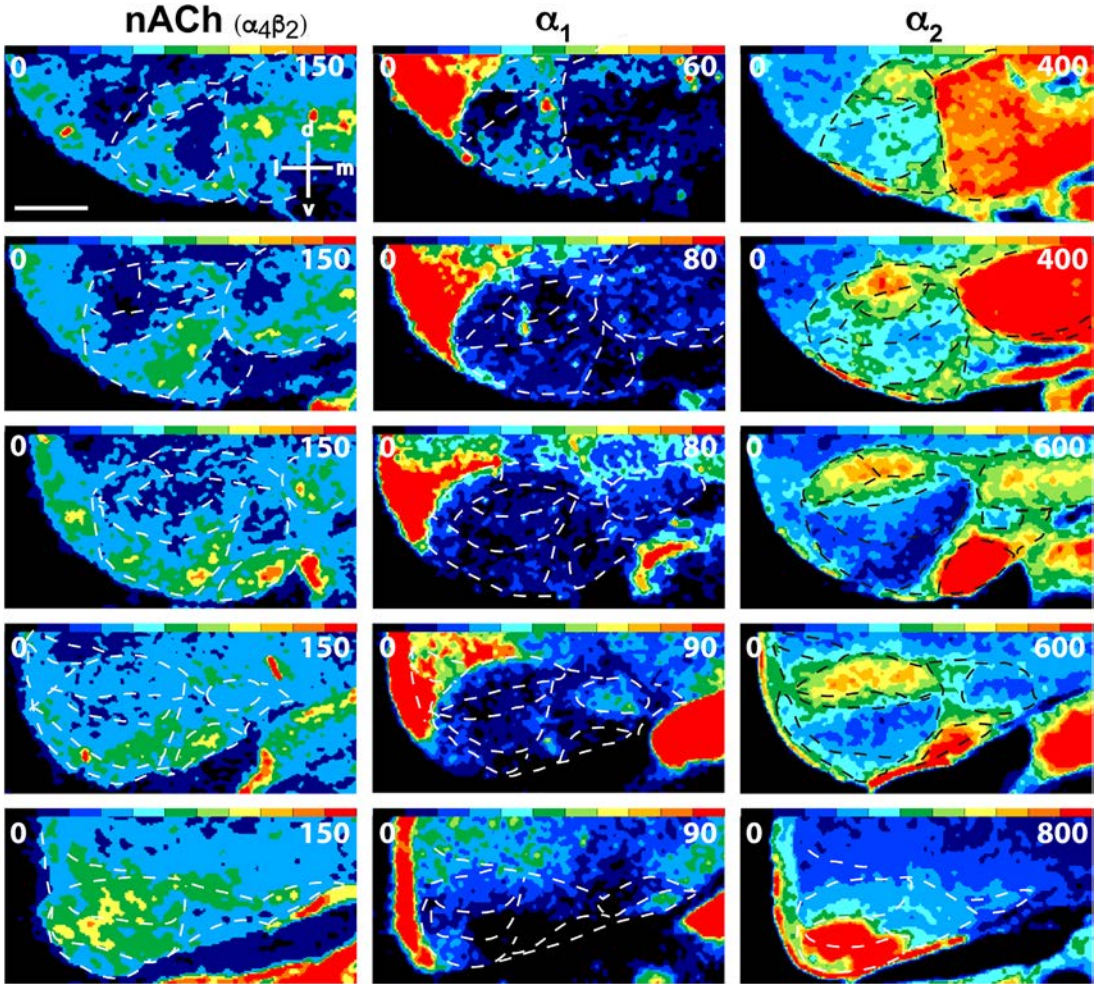

FIGURE 9 Color-coded autoradiographs showing the distribution and density of nACh receptors ($\alpha_4\beta_2$ subtype) and noradrenergic receptors at different rostro-caudal atlas levels of a series of five cross sections with a gap of approximately 500 μm between each slice of the arcopallium/amygdala complex. Left column: nACh ($\alpha_4\beta_2$ subtype) receptor expression in the arcopallium/amygdala complex from anterior (top) to posterior (down) levels. Middle column: α_1 receptor expression in the arcopallium/amygdala complex from anterior (top) to posterior (down) levels. Right column: α_2 receptor expression in the arcopallium/amygdala complex from anterior (top) to posterior (down) levels. Further explanations see Figure 7 [Color figure can be viewed at wileyonlinelibrary.com]

that functionally PoAb and AM belong to the viscero-limbic network, while AV is involved in auditory-associative processing (Shanahan et al., 2013). The second Cluster II comprises two groups, the posterior LSt and SpA, two subpallial structures that were recognized earlier as functionally closely related as caudal LSt (CLSt) and SpA (Abellán & Medina, 2009; Kuenzel et al., 2011). The second subgroup in Cluster II comprises AA, AD, AI that are more centrally located in the arcopallium and adjacent to each other. All three subdivisions are of pallial origin and have premotor-associative functions (Shanahan et al., 2013). We will now discuss these findings in more detail for each subregion below.

In the past, the arcopallium anterius (AA) was considered to be a trigeminal component because of its connectivity to the tractus fronto-arcopallialis and the anterior commissure (Schall, Güntürkün, & Delius, 1986; Wild, Arends, & Zeigler, 1984; Zeier & Karten, 1971). Therefore, together with AD and AI, AA was located in the high level associative module within the premotor submodule of the "structural connectome" in the telencephalon of the pigeon (Shanahan et al., 2013). In our receptor study, all three arcopallial subdivisions were also in the same cluster if the overall receptor densities were analyzed. Based on a study that measured the Euclidian distance of diverse mRNA expression levels within different subregions of the arcopallium in the zebra finch (*Taeniopygia guttata*), AA seems to differ from all other nuclei in this area (Jarvis et al., 2013). This does not match the current analysis based on receptor binding densities as confirmed by our cluster analysis. One explanation could be species differences in brain subdivisions or gene expression. However, it could be also possible that in vocal learning birds the arcopallium is located more medial in the forebrain and somewhat rotated medially compared to other avian species (Wang et al., 2015). Thus, it is possible that what is anterior arcopallium in the zebra finches could be more anterior-medial in pigeons, or in some other position.

Arcopallium dorsale (AD) was clearly labeled by the expression of α_2, M_1, and M_2 receptors, which is comparable to the results of former autoradiography studies in birds (Ball, Nock, Wingfield, McEwen, &

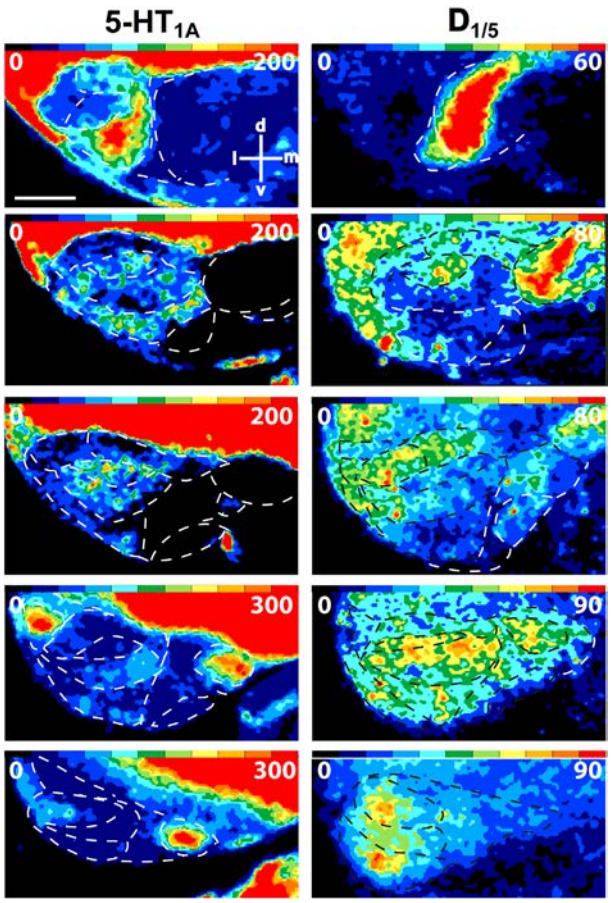

FIGURE 10 Color-coded autoradiographs showing the distribution and density of 5-HT_{1A} and $D_{1/5}$ receptors at different rostro-caudal atlas levels of a series of five cross sections with a gap of approximately 500 μm between each slice of the arcopallium/amygdala complex. Left column: 5-HT_{1A} receptor expression in the arcopallium/amygdala complex from anterior (top) to posterior (down) levels. Right column: $D_{1/5}$ receptor expression in the arcopallium/amygdala complex from anterior (top) to posterior (down) levels. Further explanations see Figure 7 [Color figure can be viewed at wileyonlinelibrary.com]

Balthazart, 1990; Herold et al., 2011; Kohler, Messer, & Bingman, 1995). AD was defined earlier by Nissl staining, tract-tracing, neurochemical and immunohistochemical studies (Atoji et al., 2006; Atoji & Wild, 2009; Herold et al. 2012; Karten & Hodos, 1967; Kröner & Güntürkün, 1999; Reiner et al., 2004; Yamamoto & Reiner, 2005). Based on our results, the receptor profile of AD showed a closer similarity to AA and AI, and is more different from AV, AM and AP. Other studies that used in situ hybridization further observed relatively high D_{1A} receptor mRNA labeling in AD in seven day old chicks (*Gallus gallus*), but low D_{1B} receptors (Sun & Reiner, 2000) and high D_{1C} mRNA levels in zebra finch (Jarvis et al., 2013). Despite the fact that the $D_{1/5}$ receptor ligand used here labels D_{1A} and D_{1B} (and possible $D_{1C/D}$) receptors together, adult expression levels of DA receptors may differ from hatchlings, which may result in lower densities in adults. This was also observed for mRNA expression profiles of different D_1 receptor types in the arcopallium of zebra finches, which tend to lower expression levels in adults compared to hatchlings (Kubikova et al., 2010). For the first time, we described a further sub-differentiation of AD, based on the observed distinct fiber architecture of ADl and ADm, particularly in the more anterior portions. Four different receptor subtypes confirmed such an intranuclear subdivision. Based on its known connectivity AD is considered to be premotor in its nature (Zeier & Karten, 1971; Shanahan et al., 2013). However, the dorsal arcopallium showed intense LAMP labeling which would go along with limbic functions (Yamamoto & Reiner, 2005). Intense LAMP labeling of AD is in line with connectivity studies that showed inputs to AD from limbic regions like the piriform cortex, hippocampal formation and TnA, and outputs to the limbic medial and somatic lateral striatum (Bingman et al., 1994; Veenman et al., 1995; Atoji & Wild, 2006). Recently reported visual stimulus selective neurons in AD, however questions both, the limbic and the premotor nature of AD (Scarf et al., 2016). However, at this time point, none of the analysis seems to be sufficient to explain the di(tri)chotomy of AD.

Arcopallium intermedium (AI) could be separated from the neighboring regions AD, AV, and AM by many differences in receptor expression, underlining the neurochemical diversity of these two arcopallial regions. Comparable to our findings, in chickens higher α_2 receptors were reported in AM compared to AI (Diez-Alarcia, Pilar-Cuellar, Paniagua, Meana, & Fernandez-Lopez, 2006). In the zebra finch brain, expression analysis of different mRNAs for kainate receptors showed higher amounts of RA, in the intermediate arcopallium if compared to the rest of the arcopallium, while AMPA receptor mRNAs showed lower amounts (Wada et al., 2004). Further, while NR2A receptor subunit is higher expressed in RA, other subunits were lower expressed, which in sum would possibly result in similar levels of NDMA receptors if measured together in all arcopallial structures. Here we found lower kainate levels of AI compared to other arcopallial structures, except AP, which is in sum in contrast to the above-mentioned study. In our study, further lower or similar amounts of AMPA receptors were detected, and lower, similar or higher densities of NMDA receptors in the different arcopallial subdivision were shown, which would be in sum possibly in line with the expression study (Wada et al., 2004). However, the caveat of ligand binding studies is that most ligands bind to multiple gene products of the same gene, so that they do not have the anatomical high resolution of mRNA binding studies that provide information of distinctively expressed single gene profiles, so in general some differences between mRNA levels and overall protein levels may exist. Further, to some extent, mRNA levels may differ in general from protein levels. Several previous studies have reported intra-nuclear subregions for AI (Atoji & Wild, 2009; Kröner & Güntürkün, 1999; Shanahan et al., 2013; Wynne & Güntürkün, 1995; Zeier & Karten, 1971). However, no consistent view could be established. In our receptor analysis, the significant differences were observed between a dorsal and a ventral component of AI in 6 out of 11 measured receptors. This was particularly visible for the muscarinergic receptors. Additionally, the cellular as well as fiber architecture of AId and AIv differed. AI is a major hub of the "structural connectome" of the telencephalon of the pigeon and as mentioned above, located in the associative module and premotor submodule (Shanahan et al., 2013). This means that AI

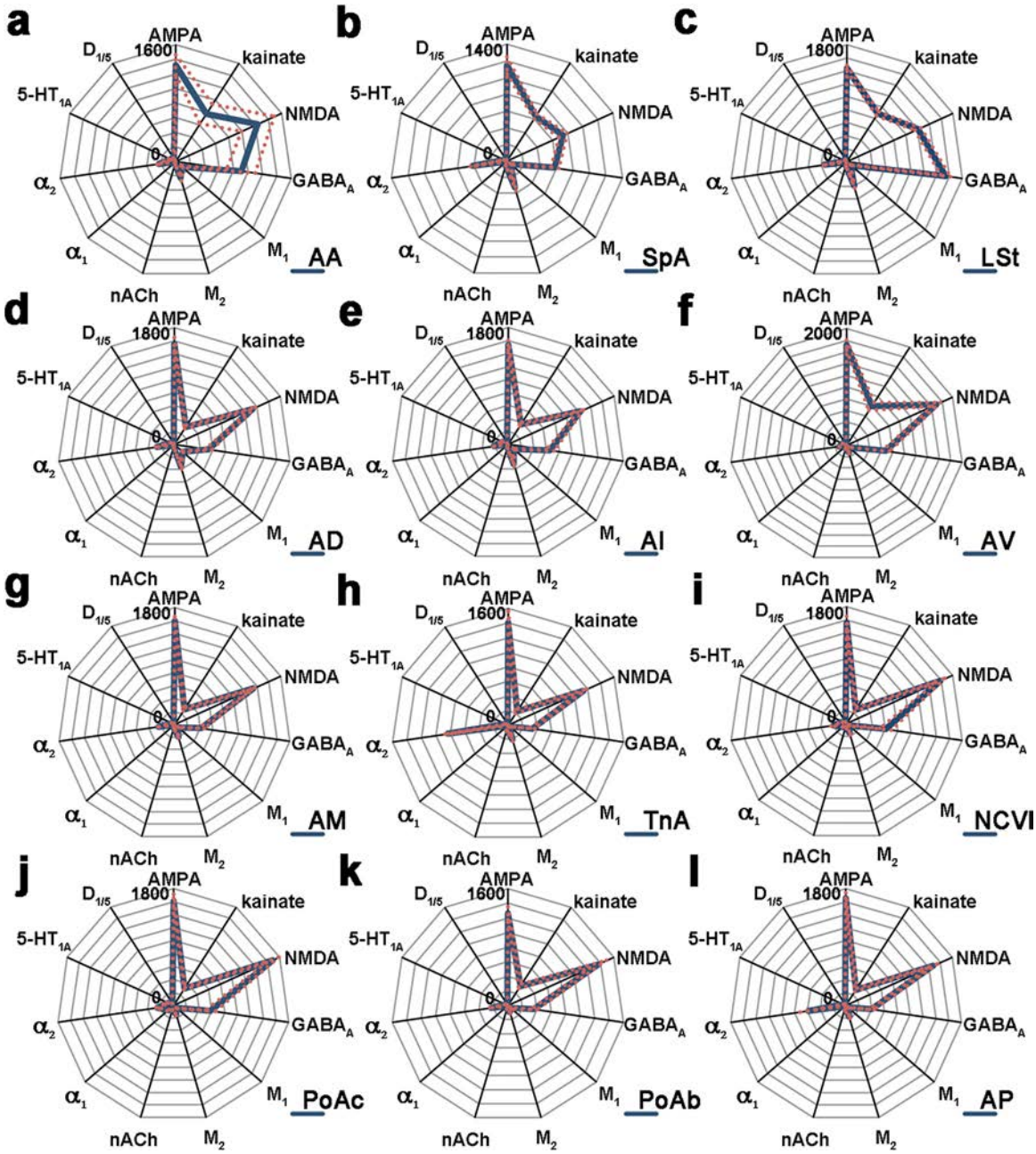

FIGURE 11 Receptor fingerprints of the subregions defined within pigeon arcopallium/amygdala complex, the lateral striatum and the nidopallium caudoventrale pars lateralis (a–l). The coordinate polar plots show the different mean receptor densities in fmol/mg protein for the arcopallial and amygdala subregions and adjacent regions. Blue lines connecting the mean densities of the 11 receptors in each subregion define the shape of the fingerprint. Light red dotted lines represent the standard errors of means of the different receptor densities in each region. Note that the scales in (a–l) are different. For abbreviations see list [Color figure can be viewed at wileyonlinelibrary.com]

innervates pallial, diencephalic and brain stem entities and at the same time receives input from associative, multimodal structures in the nidopallium and the dorsolateral region of the hippocampal formation, and from visual associative subregions of the hyperpallium and from many more (see Shanahan et al., 2013 for review).

Arcopallium ventrale (AV) showed the highest concentrations of glutamate receptors of the arcopallium/amygdala complex and high kainate receptor densities nicely resolved the borders of AV, which would be comparable to the reported high mRNA levels of kainate receptors of Ai in zebra finches (Wada et al., 2004) that was not separated into Ai and Av in the study of Wada and colleagues. However, differences between RA and the region ventral to RA in the zebra finch were mentioned in a recent study (Olson, Hodges, & Mello, 2015). In the pigeon, AV showed further substantial differences in various receptor densities, cell densities and fiber architectural details if compared to the surrounding AI, PoAb, and AM. Thus, it could be recognized as a separate

The Journal of Comparative Neurology

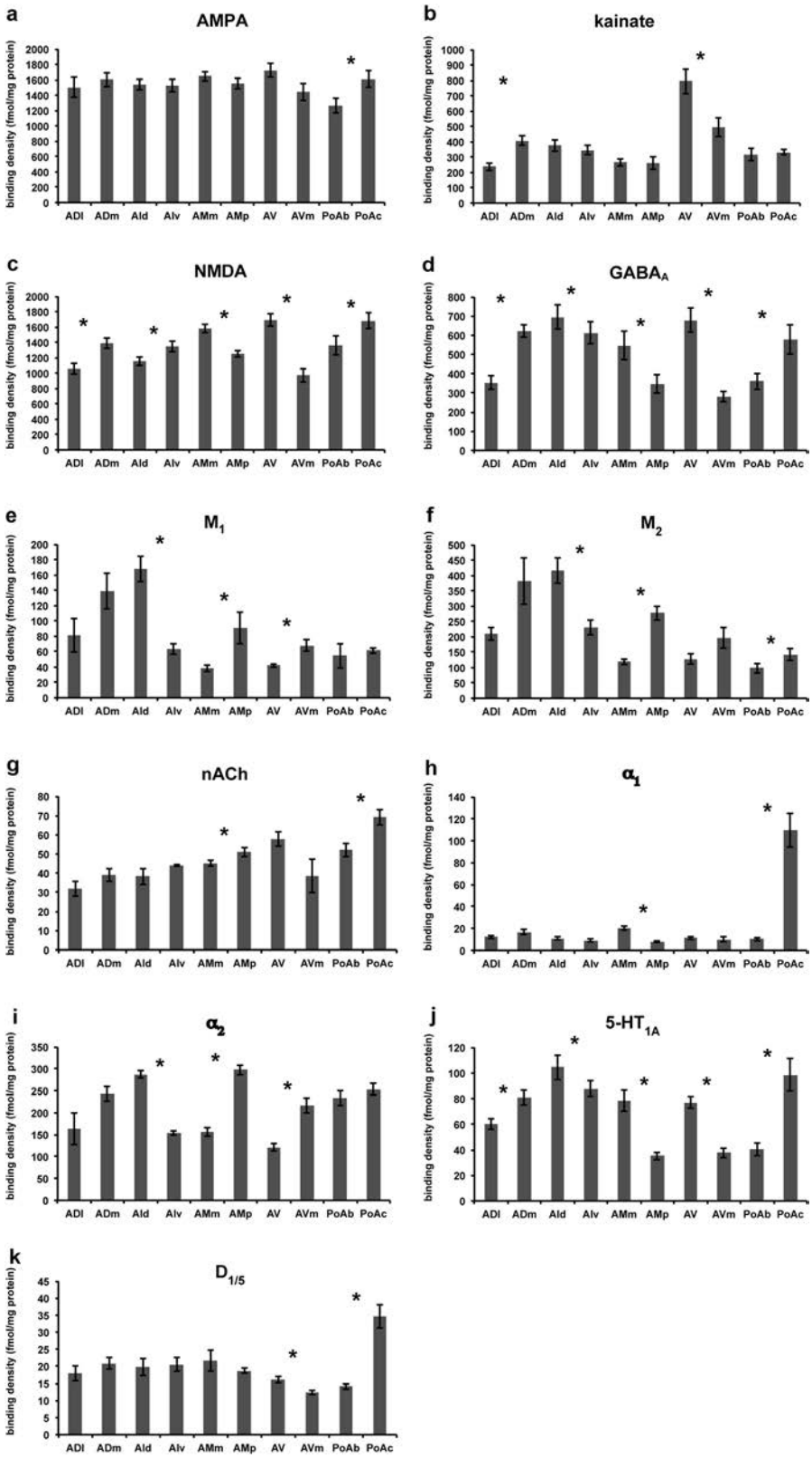

FIGURE 12 Histograms of the mean receptors densities (fmol/mg protein) of intra-nuclear substructures of the pigeon arcopallium/amygdala complex (a–k). PoA and AV showed the highest numbers of receptor density differences between the intra-nuclear substructures PoAc and PoAb or AV and AVm. NMDA, $GABA_A$, and $5\text{-}HT_{1A}$ receptors confirmed all intra-nuclear substructures. Error bars represent standard errors of the means. Asterisks represent significant differences between intra-nuclear substructures of an examined subregion ($p < .05$; *Wilcoxon-rank test*). For abbreviations see list

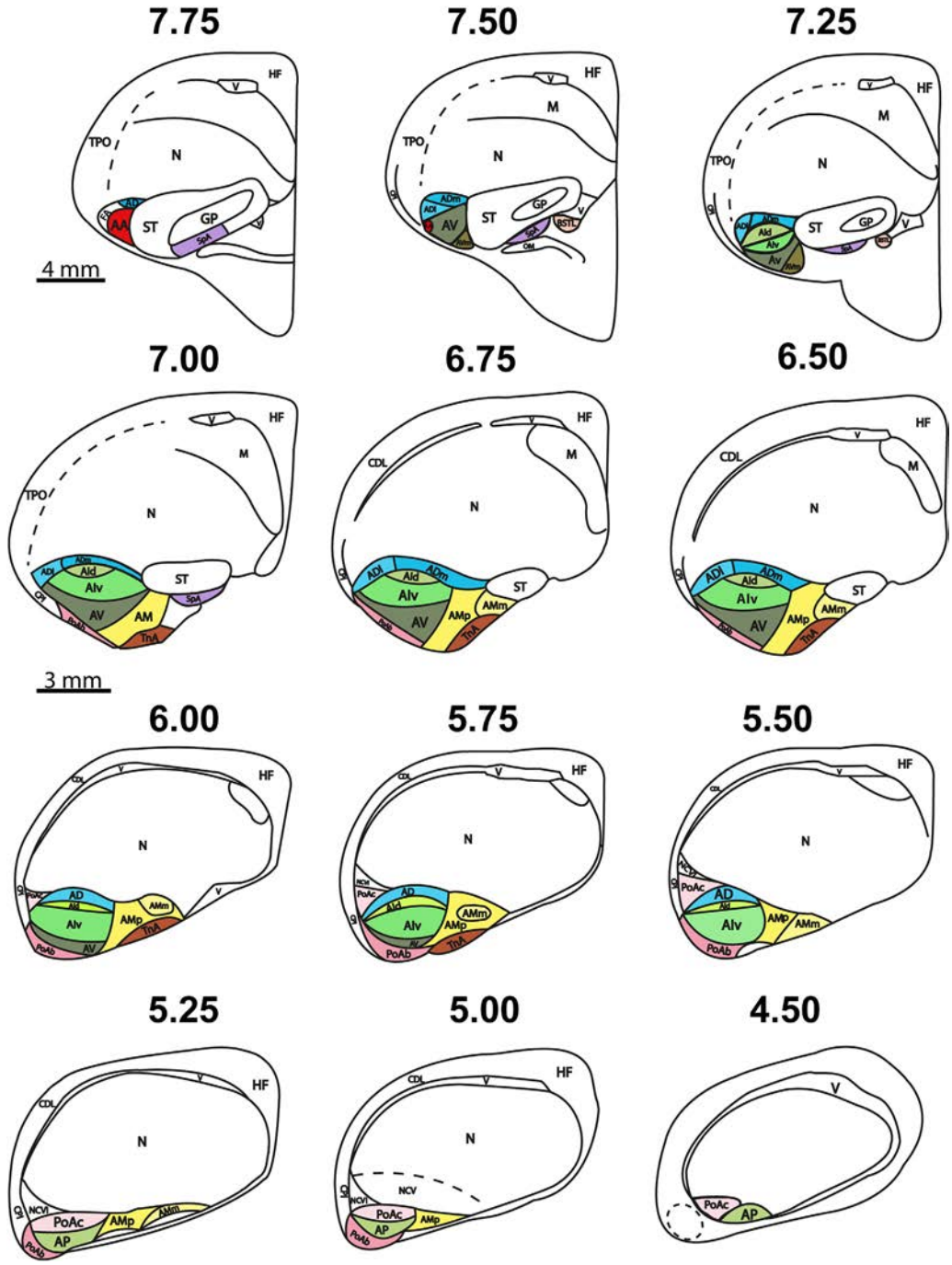

FIGURE 13 Schematic atlas of the arcopallium/amygdala complex in serial frontal sections. The atlas map is based on differences in the cyto-, myelo-, and receptor-architecture. Atlas levels correspond to the rostro-caudal atlas levels A 7.75 to A 4.50 (Karten & Hodos, 1967). For abbreviations see list [Color figure can be viewed at wileyonlinelibrary.com]

arcopallial region. Our results were supported by findings from tracing studies and further analysis of connectivity, which described AV as different from AI (Atoji & Wild, 2004; Kröner & Güntürkün, 1999; Shanahan et al., 2013; Wild, Karten, & Frost, 1993). In the more anterior portion of AV an intranuclear subregion was recognized that we named AVm. AVm showed different densities in 8 out of 11 receptors. Atoji and Wild (2009) showed that both the limbic central caudal nidopallium (NCC) and the dorsal intermediate mesopallium have tight connections with a structure named AIvm that is located in about the same location as our AVm. In a prior publication, Wild and colleagues (1993), however, had proposed AIvm to be part of an auditory premotor structure. According to Shanahan et al. (2013), AV could be an associative structure that is part of the avian prefrontal submodule, while AIvm is located in the auditory module. Like AA, AV projects via the anterior commissure to the contralateral arcopallium (Letzner et al., 2016).

Arcopallium mediale (AM) was first described in a study of Zeier and Karten (1971). Later on, tract-tracing experiments confirmed its existence and a detailed analysis of the cytoarchitecture with Nissl

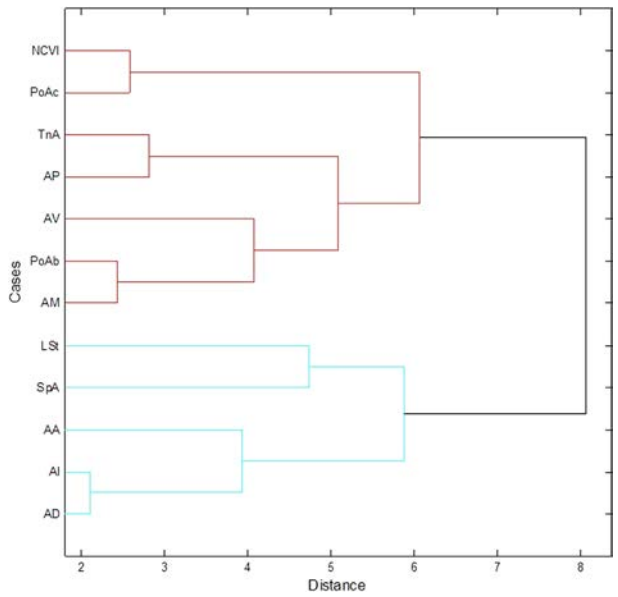

FIGURE 14 Relationships of the overall mean receptor densities between subregions of the amygdala, the arcopallium, the nidopallium caudolaterale pars lateralis and the posterior lateral striatum. X-axis: Euclidian distance. Y-axis: Subregions. The cladogram shows two different main clusters with further subgroups at different branches (cophenetic correlation coefficient $c = 0.60$) [Color figure can be viewed at wileyonlinelibrary.com]

staining offered a more precise definition of the AM in pigeons (Atoji et al., 2006). The AM is divided into a medially located cell-dense, dark stained division with large cells (AMm) and a less cell-dense, parvocellular division (AMp) located laterally (Atoji et al., 2006). In our study, the borders of AM are identical to the studies of Atoji and colleagues (2006, 2009) and fibers showed different densities and directions in both subnuclei. Tracing studies have shown that AM projects extensively to PoAc and to a lesser extent to BSTL (Atoji et al., 2006). In a follow-up study by Atoji and Wild (2009), it was shown that the central caudal nidopallium (NCC) has reciprocal connections with AMm and AMp. Both areas are associated with neuroendocrine and autonomic functions in various bird species and have connections to TnA and the postero-medial hypothalamus via HOM (Cheng, Chaiken, Zuo, & Miller, 1999; Cohen, 1975; Thompson, Goodson, Ruscio, & Adkins-Regan, 1998; Zeier & Karten, 1971). The ventrolateral part of AMp together with AIvm from Wild and colleagues (1993) were called Avpm in Zeier and Karten (1971) and based on their connectivity pattern are limbic-associated. Additionally, the overall receptor architecture of AM seemed to be more comparable to limbic regions as confirmed by the cluster analysis.

Arcopallium posterioris (AP) is the most caudal part of the arcopallium and is positioned between atlas levels A5.25 and A4.50. In line with other studies, we recognized this differentiation of PoAc, PoAb and the arcopallium intermedium in the more posterior sections based on our receptor data as well as cyto- and myelo-architecture. This area was described earlier in pigeons as the most posterior part of Al (Atoji et al., 2006) and with gene expression and cellular analysis in zebra finches (Jarvis et al., 2013). In zebra finches Ap is enriched in D_1 receptors (Jarvis et al., 2013), while here D_1 receptor expression of AP was only higher if compared to AV. As mentioned above, overall receptor densities of AP showed more similarities to TnA than to other arcopallial regions. Future studies and possibly a more detailed analysis of other gene expression profiles in the pigeon have to find out how this relationship may be interpreted and to which functional circuit AP is belonging.

Nucleus posterioris amygdalopallii (PoA) can be separated into a basal (PoAb) and a compact part (PoAc). All researchers agree that this nucleus is part of the avian amygdala (Reiner et al., 2004). A higher cell density defines PoAc, while PoAb shows a smaller number of cells with greater cell bodies (Atoji et al., 2006). This is particularly visible at the atlas level A5.00. The analysis of the receptor autoradiographs confirmed differences between PoAc and PoAb, thereby supporting a separation of these two nuclei. The highest divergences between PoAc and PoAb were detected for α_1, 5-HT_{1A}, and $D_{1/5}$ receptors. For example, PoAc showed two-times higher densities of $D_{1/5}$-receptors and 11-times higher densities of α_1 receptors. This is in line with the findings that PoAc is also characterized by high tyrosine hydroxylase (TH) immunoreactivity, while PoAb has more or less no TH positive cells (Kröner & Güntürkün, 1999). PoAb, but not PoAc participates in interhemispheric projections via the anterior commissure, a result that underlines the difference of these two subnuclei (Letzner et al., 2016). The region overlaying PoAc is named NCVl. It can be distinguished by the absence of TH immunoreactivity and darkly stained cell aggregates (Atoji et al., 2006; Kröner & Güntürkün, 1999; Wild, Arends, & Zeigler, 1985). PoAc and PoAb showed differences in receptor densities from the overlaying NCVl. NCVl together with the subnidopallium were discussed to be a part of the insular cortex (Atoji et al., 2006) or to form the endopiriform nucleus (Yamamoto & Reiner, 2005). Atoji and colleagues (2006) further analyzed and defined the borders of limbic BSTL at the ventral tip of the lateral ventricle more precisely and showed extensive connections to PoAc but not to PoAb in birds (Atoji et al., 2006). PoAb on the other hand is connected to CDL and TPO (Atoji & Wild, 2005). Both, PoAc and BSTL receive fibers from the dorsomedial subregion of the hippocampal formation (HF) but send only a small number of efferent fibers to the dorsomedial and the dorsolateral region of the HF (Atoji & Wild, 2004). In addition, AM projects extensively to PoAc and to a lesser extent to BSTL (Atoji et al., 2006). As mentioned above, PoA and NCVl belong to the viscero-limbic module in the pigeon's connectome (Shanahan et al., 2013).

Nucleus taenia amygdala (TnA) is considered to be amygdaloid and subpallial (Reiner et al., 2004). However, the subpallial nature of TnA has been questioned by some researchers of the avian brain consortium (Reiner et al., 2004), which is further underlined by our cluster analysis. Future studies have to be performed to bring more clarity at this point. No clear subdifferentiation of TnA was recognized although this was mentioned in other studies in chickens and budgerigars (*Melopsittacus undulates*; Roberts, Hall, & Brauth, 2002; Yamamoto et al., 2005). TnA is specifically visible by labeling of M_2 and α_2 receptors. A high α_2 receptor binding of TnA was also reported in Fernandez-Lopez et al. (1997) and visible in Herold et al. (2011). Generally, TnA showed a high number of differences in receptor densities if

compared to other subregions of the arcopallium/amygdala complex. This distinction had already been identified using immunostaining in various bird species (de Lanerolle, Elde, Sparber, & Frick, 1981; Deviche & Güntürkün, 1992; Martinez-Vargas, Stumpf, & Sar, 1976; Roberts et al., 2002). Based on its connections to the hippocampal formation, the olfactory bulb (Casini, Bingman, & Bagnoli, 1986; Reiner & Karten, 1985; Székély & Krebs, 1996) and its role in social behavior (Cheng et al., 1999), TnA had always been discussed as part of the avian amygdala. This is strengthened by the additional connections of TnA to the hypothalamus, the septal region, the medial striatum, the hyperpallium, and the nidopallium caudolaterale (Cheng et al., 1999; Leutgeb, Husband, Riters, Shimizu, & Bingman, 1996; Zeier & Karten, 1971). TnA was included in the septo-hippocampal network of the pigeon's telencephalic connectome (Shanahan et al., 2013).

Area subpallialis amygdala (SpA) was separated from neighboring structures AM and posterior LSt by distinct receptor densities. SpA is considered to belong to the extended amygdala and is basically defined by its different neurochemistry and connectivity as a region ventral to the globus pallidus at the level of OM (Reiner et al., 2004; Yamamoto et al., 2005). The overall receptor analysis indicated a similarity between SpA and posterior LSt that has to be further investigated in future studies, but as mentioned above was also recognized in the past (Abellán & Medina, 2009).

4.3 | General comparisons of the avian amygdala complex to the mammalian amygdala

The mammalian amygdala is molecularly and structurally heterogeneous, comprising lateral and ventral pallial parts and striatal and pallidal subpallial portions, which can be extended rostrally (Puelles et al., 2000). The pallial subregions comprise the lateral (LA), basolateral (BLA), basomedial (BM) and cortical nuclei (CoA) of the amygdala, and the subpallial subregions comprise the central (CeA) and medial nuclei of the amygdala (MeA) (Sah, Faber, Lopez De Armentia, & Power, 2003; Swanson & Petrovich, 1998). As described above, in birds, PoAc, PoAb, TnA, SpA, and BSTL are considered to form the avian amygdala.

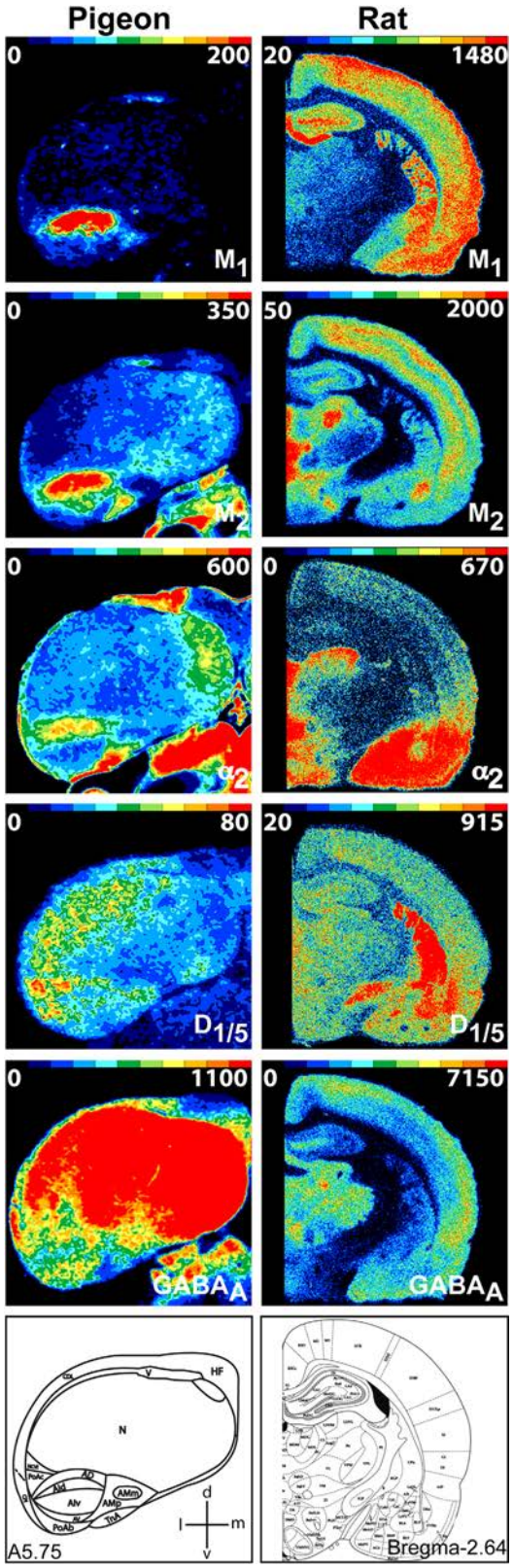

FIGURE 15.

FIGURE 15 Comparisons of different receptors between the pigeon arcopallium/amygdala complex around atlas level A 5.75 (left column) and the rat amygdala complex/cortical areas around atlas level bregma -2.16 (Paxinos and Watson, 2005; right column). Pigeon: for abbreviations see list. Rat: AIP, posterior agranular insular cortex; BLA, basolateral amgydaloid nucleus, anterior part; BLP, basolateral amgydaloid nucleus, posterior part; BLV, basolateral amgydaloid nucleus, ventral part; BMA, basomedial amgydaloid nucleus, anterior part; BMP, basomedial amgydaloid nucleus, posterior part; CPu, Caudate/Putamen; CeC, central amygdaloid nucleus, capsular part; CeM, central amygdaloid nucleus, medial division; CeL, central amygdaloid nucleus, lateral division; DI, dysgranular insular cortex; GI, granular insular cortex; LAVL, lateral amygdaloid nucleus, ventrolateral part; LAVM, lateral amygdaloid nucleus, ventromedial part; M1, primary motor cortex, M2, secondary motor cortex; MeAD, medial amygdaloid nucleus anterodorsal part; MePD, medial amygdaloid nucleus posterodorsal part; MePV, medial amygdaloid nucleus posteroventral part; S1, primary somatosensory cortex; S2, secondary somatosensory cortex; STIA, bed nucleus of the stria terminalis, intra-amygdaloid division [Color figure can be viewed at wileyonlinelibrary.com]

PoA: Genoarchitecture and fate mapping studies in diverse species revealed that PoA expressed various pallial markers and is therefore considered to be part of the pallial amygdala in birds (Puelles et al., 2000; Reiner et al., 2004; Puelles et al., 2007; Abellán & Medina, 2008; Abellán et al., 2009, 2010; Butler et al., 2011; Medina et al., 2011; Kuenzel et al., 2011). The projections of PoAc showed a comparable connectivity pattern of commissural fibers to the mammalian amygdala, which projects contralaterally to cortical, medial, and lateral nuclei of the amygdala, olfactory tubercle and pre-piriform cortex (De Olmos & Ingram, 1972; Letzner et al., 2016; Sah et al., 2003). However, PoAc shares connectional characteristics of both, the autonomic and the fronto-temporal system of mammals and thus with both the central and the basolateral/lateral nuclei of the mammalian amygdala (Veenman et al., 1995; Swanson & Petrovich, 1998; Puelles et al., 2000; Atoji et al., 2006). Here, PoAc showed the high amounts of α_1, 5-HT_{1A} and $D_{1/5}$ receptors compared to the other amygdala subregions. In rodents, α_1, α_2, and $D_{1/5}$ receptors are densely expressed in the amygdala, and in humans in LA and BLA (Cremer et al., 2010; Cremer et al., 2009; Lillethorup et al., 2015; Sanders et al., 2006). Further, α_1 receptors showed higher densities in LA compared to BLA in humans (Graebenitz et al., 2011). The most striking differences within the mouse amygdala complex were reported for M_1 receptors densities showing higher amounts in the lateral region compared to the medial and central nucleus (Yilmazer-Hanke, Roskoden, Zilles, & Schwegler, 2003). In pigeons, M_1 receptors were higher expressed in PoAb, PoAc, SpA compared to TnA. Further, PoAc and PoAb express higher numbers of NMDA receptors that are also densely expressed in the lateral and medial regions compared to the central region in mice (Yilmazer-Hanke et al., 2003). Further, TH-positive fibers and the absence of acetylcholine-esterase immune-reactivity define LA in rats (Paxinos, Kus, Ashwell, & Watson, 1999). TH-positive fibers were also reported for PoAc (Kröner & Güntürkün, 1999). Taken together, no unitary pattern could be observed, but at least PoAc showed some similarities in the receptor expression profile of the mammalian lateral regions of the amygdala.

TnA: Based on their similarities in olfactory input, hippocampal, and hypothalamic output, enrichment in androgen and estrogen receptors and involvement in sexual behavior, TnA was considered to be comparable to the MeA of mammals (Reiner et al., 2004; Yamamoto et al., 2005). It has been speculated that lateral TnA in chickens (pallial) is comparable to the anterior division of the corticoid nucleus of the amygdala (CoAa), whereas medial TnA (subpallial) is comparable to MeA (Roberts et al., 2002; Yamamoto et al., 2005; Yamamoto & Reiner, 2005). However, we did not observe this subdifferentiation of TnA in pigeons. TnA showed very high amounts of α_2-receptors that are also densely expressed in the pallial as well as subpallial nuclei of the amygdala (MeA, LA, and BLA) of mice, rats and humans if compared to cortical probes (Graebenitz et al., 2011; Lillethorup et al., 2015; Sanders et al., 2006; Scheperjans, Grefkes, Palomero-Gallagher, Schleicher, & Zilles, 2005; Scheperjans, Palomero-Gallagher, Grefkes, Schleicher, & Zilles, 2005).

Extended amygdala: In mammals, some researchers divide the subpallial amygdaloid nuclei (including the extended amygdala) into the central and medial extended amygdala complex (Kuenzel et al., 2011). The central extended amygdala complex consists of the CeA and BSTL and the medial extended amygdala complex consists of MeA and BSTM. Both, CeA and MeA are the major output nuclei of the amygdala and confluent with the BST nuclei (Swanson, 2000). Comparative studies in chick and mouse embryo with subpallial and pallial genetic markers, as well as connectivity data suggests that the BST nuclei BSTM and BSTL in birds belong to the extended amygdala nuclei (Abellán & Medina, 2008, 2009; Abellán, Menuet, Dehay, Medina, & Retaux, 2010; Bruce, Erichsen, & Reiner, 2016; Butler et al., 2011; Medina et al., 2011; Puelles et al., 2000; Puelles et al., 2007). In birds, it has been further postulated that SpA and BSTL form the central extended amygdala complex, while TnA and BSTM form another functional unit and may correspond to the medial extended amygdala complex (Puelles et al., 2000; Reiner et al., 2004; Abellán & Medina, 2009; Kuenzel et al., 2011). To test these hypotheses, researchers investigated secretagogin-binding that selectively labels the subpallial and extended amygdala in mammals (Gati, Lendvai, Hokfelt, Harkany, & Alpar, 2014; Mulder et al., 2010). In chickens, TnA, SpA and the BNST nuclei were densely populated with secretagogin-positive neurons. However, the pallial amygdala PoA as well as AV and AD also contained labeled neurons, which questions the use of this marker as subpallial-specific in birds. On the other hand, analysis of the connections of BSTL strongly supports the idea that BSTL belong to the extended amygdala in birds (Atoji et al., 2006; Veenman et al., 1995). SpA has been suggested to be comparable to the sublenticular part of the mammalian extended amygdala (Yamamoto & Reiner, 2005; Kuenzel et al., 2011). Both structures show similarities in location (ventral to GP), connections with the parabrachial area, the nucleus of the solitary tract, the dorsal motor nucleus of the vagus, the arcopallium, efferents to the BSTL (Atoji et al., 2006; Reiner et al., 2004; Wild, Arends, & Zeigler, 1990) as well as neurotransmitter traits such as enrichment in CGRP immunopositive fibers, enkephalinergic, and neurotensinergic neurons (Atoji, Shibata, Yamamoto, & Suzuki, 1996; Lanuza, Davies, Landete, Novejarque, & Martinez, 2000; Yamamoto et al., 2005). In our study, SpA showed the lowest densities of NMDA receptors. Lower NMDA receptors were also observed in the mice central amygdala if compared to the lateral and medial nuclei (Yilmazer-Hanke et al. 2003), which would fit with recent theories that SpA is part of the central extended amygdala complex (Vicario et al., 2014). On the other hand, the central nucleus in mice is also conspicuously low in $GABA_A$ receptors (Yilmazer-Hanke et al., 2003), while the lowest amounts of $GABA_A$ receptors in the pigeon amygdala subregions were detected in PoAb and TnA.

4.4 | General comparisons of the avian arcopallium complex to mammalian (pre)-motor cortical areas

The arcopallial subregions of birds are considered to be functionally comparable to (pre)motor cortical areas by some researchers (Reiner et al., 2004; Jarvis et al., 2005; Chen et al., 2013; Whitney et al., 2014; Pfenning et al., 2014; Karten, 2015; Güntürkün & Bugnyar, 2016), while others still assume that all arcopallial regions belong to the

amygdala (Puelles et al., 2000, 2007; Medina et al., 2011; Bupesh et al., 2011). In pigeons the arcopallial subregions receive input from the NCL, the functional analog of the mammalian prefrontal cortex (Güntürkün & Bugnyar, 2016; Herold, Diekamp, & Güntürkün, 2008; Herold, Joshi, et al., 2012; Leutgeb et al., 1996), as well as auditory (Wild et al., 1993), trigeminal (Wild et al., 1985), somatosensory (Kröner & Güntürkün, 1999) and visual pallial areas (Husband & Shimizu, 1999). Based on layer-specific gene expression analysis and cell type homologies Dugas-Ford and colleagues (2012) postulated that regions of the arcopallium are comparable to layer V neurons of the neocortex. One example, ER81 showed homogeneous labeling throughout the whole zebra finch arcopallium, including RA. Another marker, PCP4, showed intense labeling of subregions in chicken and zebra finch that correspond to AD and AId in our study. However, PCP4 and ER81 are also expressed in the basolateral amygdala of mammals, a pallial derivative, and not exclusively in layer V neurons (Jarvis et al., 2013; Nomura, Hattori, & Osumi, 2009). One explanation for this could be that the pallial amygdala is an extension of cortex layers V and VI, and therefore shares the expression of the same marker genes (Swanson, 2000). A more extensive gene expression pattern analysis by Pfenning and colleagues (2014) revealed for nearly thousand genes a close functional similarity of RA and the surrounding intermediate arcopallium in songbirds with the primate primary motor cortex. A cell type specific analysis from different layers in motor and sensory cortices, showed that layer V cells of macaque (*Macaca mulatta*) primary motor cortex had the strongest match with RA and surrounding arcopallium compared to all other layers and sensory cortex (Pfenning et al., 2014). Further, for 55 genes, a "convergence" of RA to the human laryngeal motor and adjacent primary somatosensory cortex was found, since these genes had similarly different expression profiles from the surrounding arcopallium. Here we think that to analyze different brain regions and cell types based on expression profiles of gene orthologs and other characteristics more precisely, a detailed brain map with higher resolution is needed for better comparisons of similarities between cortical layers/areas in mammals, cortical areas in reptiles and nuclei in birds.

Our new schematic map of the arcopallium/amygdala complex allows a more precise comparison of the receptor architecture to mammalian (pre)-motor, other cortical as well as amygdala subregions. Although absolute densities of binding sites vary between different species, relative differences between regional densities are mostly comparable (Herold et al., 2015; Zilles & Palomero-Gallagher, 2016). For example, in the (pre)-motor regions of different mammalian species, NMDA and $GABA_A$ receptors showed the highest densities, and M_1/α_1 receptors were higher expressed compared to M_2/α_2 receptors (Gebhard et al., 1995; Geyer et al., 1998; Herold et al., 2011; Palomero-Gallagher, Schleicher, Zilles, & Loscher, 2010; Palomero-Gallagher & Zilles, 2004; Zilles et al., 1995). In humans, M_2 and $GABA_A$ receptors are more densely expressed in primary visual (BA17), somatosensory (BA3) and primary auditory cortex if compared to the primary motor cortex (BA4; Zilles, Palomero-Gallagher, & Schleicher, 2004; Scheperjans, Grefkes et al., 2005; Scheperjans, Palomero-Gallagher et al., 2005). Particularly the dense M_2-receptor expression seems to be a conservative aspect of cortical organization (Zilles et al. 2004). Referring to this, it is of further interest that the pallial nuclei, LA and BLA in humans and BLA in rats have high amounts of M_2-receptors (Graebenitz et al., 2011; Mash & Potter, 1986). Additionally, in humans and rats, $D_{1/5}$ receptors are higher expressed and $GABA_A$ receptors are lower expressed in the amygdala if compared to the above-mentioned cortical areas (Scheperjans, Grefkes et al., 2005; Scheperjans, Palomero-Gallagher et al., 2005; Cremer et al., 2009, 2010; Graebenitz et al., 2011). Figure 15 provides examples of the above-mentioned receptors in the rat amygdala and cortex and the pigeon arcopallium/amygdala complex that showed differences between divers subregions in mammalian species. The receptor data of relevant brain regions in rats have been published earlier (Herold et al., 2011; Cremer et al., 2009, 2010; Palomero-Gallagher & Zilles, 2004). Comparisons of relative densities of M_1, M_2, $D_{1/5,}$ α_2, and $GABA_A$ receptors between pigeons and rats support the idea that AA, AD, AI, AV, and AP share receptor expression characteristics with FR1 (M1), FR2 (M2), and the insular cortex (AIP, GI, DI). Here, high levels of $D_{1/5}$ and α_2 receptor densities of AP support the idea that AP could be comparable to AIP while dense levels of $GABA_A$, $D_{1/5}$ and M_1-receptors in AA support a comparison with FR1/FR2 and GI/DI/AIP. High $GABA_A$ receptor levels in AV point to a comparison with FR1/FR2 and AIP. In case of AI high levels of $GABA_A$, M_1, and M_2 receptors allow further comparison to FR1/FR2, S1/S2, and GI/DI/AIP. However, as visible in Figure 15 beside similar binding patterns also differences are detectable, which may be a result of parallel evolution, analogies, and species-specific adaptations.

5 | CONCLUSIONS

The pigeon arcopallium/amygdala complex is a highly heterogeneous area of the avian brain, characterized by a large number of subregions and a diversity of connectional patterns. This complexity is the reason why scientists still can't find a consensus on the number and location of subdivisions or the premotor or limbic nature of all or parts of this area. We believe that we need proper anatomical maps before embarking onto such scientific voyages. This was the motivation for our study and the reason we now present a new detailed map of this region, based on quantitative methods. In addition, our study may promote the discussions on functional similarities of premotor or limbic components, by providing details on the neurotransmitter receptor densities in pigeons in comparison with similar data in rats.

ORCID

Christina Herold http://orcid.org/0000-0002-6530-115X

REFERENCES

Abellán, A., & Medina, L. (2008). Expression of cLhx6 and cLhx7/8 suggests a pallido-pedunculo-preoptic origin for the lateral and medial parts of the avian bed nucleus of the stria terminalis. *Brain Research Bulletin*, *75* (2–4), 299–304. https://doi.org/10.1016/j.brainresbull.2007.10.034

Abellán, A., & Medina, L. (2009). Subdivisions and derivatives of the chicken subpallium based on expression of LIM and other regulatory genes and markers of neuron subpopulations during development.

The Journal of Comparative Neurology, *515*(4), 465–501. https://doi.org/10.1002/cne.22083

Abellán, A., Legaz, I., Vernier, B., Rétaux, S., & Medina, L. (2009). Olfactory and amygdalar structures of the chicken ventral pallium based on the combinatorial expression patterns of LIM and other developmental regulatory genes. *The Journal of Comparative Neurology*, *516*(3), 166–186. https://doi.org/10.1002/cne.22102

Abellán, A., Menuet, A., Dehay, C., Medina, L., & Retaux, S. (2010). Differential expression of LIM-homeodomain factors in Cajal-Retzius cells of primates, rodents, and birds. *Cerebral Cortex*, *20*(8), 1788–1798. https://doi.org/10.1093/cercor/bhp242

Ariens-Kappers, C. U., Huber, G. C., & Crosby, E. C. (1936). *The comparative anatomy of the nervous system of vertebrates, inlcuding man*. New York: MacMillan.

Atoji, Y., Saito, S., & Wild, J. M. (2006). Fiber connections of the compact division of the posterior pallial amygdala and lateral part of the bed nucleus of the stria terminalis in the pigeon (*Columba livia*). *The Journal of Comparative Neurology*, *499*(2), 161–182. https://doi.org/10.1002/cne.21042

Atoji, Y., Shibata, N., Yamamoto, Y., & Suzuki, Y. (1996). Distribution of neurotensin-containing neurons in the central nervous system of the pigeon and the chicken. *The Journal of Comparative Neurology*, *375*(2), 187–211. https://doi.org/10.1002/(SICI)1096-9861(19961111)375:2<187::AID-CNE2>3.0.CO;2-Z

Atoji, Y., & Wild, J. M. (2004). Fiber connections of the hippocampal formation and septum and subdivisions of the hippocampal formation in the pigeon as revealed by tract tracing and kainic acid lesions. *The Journal of Comparative Neurology*, *475*(3), 426–461. https://doi.org/10.1002/cne.20186

Atoji, Y., & Wild, J. M. (2005). Afferent and efferent connections of the dorsolateral corticoid area and a comparison with connections of the temporo-parieto-occipital area in the pigeon (*Columba livia*). *The Journal of Comparative Neurology*, *485*(2), 165–182. https://doi.org/10.1002/cne.20490

Atoji, Y., & Wild, J. M. (2006). Anatomy of the avian hippocampal formation. *Reviews in the Neurosciences*, *17*(1–2), 3–15.

Atoji, Y., & Wild, J. M. (2009). Afferent and efferent projections of the central caudal nidopallium in the pigeon (*Columba livia*). *The Journal of Comparative Neurology*, *517*(3), 350–370. https://doi.org/10.1002/cne.22146

Atoji, Y., & Wild, J. M. (2012). Afferent and efferent projections of the mesopallium in the pigeon (*Columba livia*). *The Journal of Comparative Neurology*, *520*(4), 717–741. https://doi.org/10.1002/cne.22763

Ball, G. F., Nock, B., Wingfield, J. C., McEwen, B. S., & Balthazart, J. (1990). Muscarinic cholinergic receptors in the songbird and quail brain: A quantitative autoradiographic study. *The Journal of Comparative Neurology*, *298*(4), 431–442. https://doi.org/10.1002/cne.902980405

Belgard, T. G., Montiel, J. F., Wang, W. Z., Garcia-Moreno, F., Margulies, E. H., Ponting, C. P., & Molnar, Z. (2013). Adult pallium transcriptomes surprise in not reflecting predicted homologies across diverse chicken and mouse pallial sectors. *Proceedings of the National Academy of Sciences of the United States of America*, *110*(32), 13150–13155. https://doi.org/10.1073/pnas.1307444110

Bingman, V. P., Casini, G., Nocjar, C., & Jones, T. J. (1994). Connections of the piriform cortex in homing pigeons (*Columba livia*) studied with fast blue and WGA-HRP. *Brain, Behavior and Evolution*, *43*(4–5), 206–218.

Bruce, L. L., Erichsen, J. T., & Reiner, A. (2016). Neurochemical compartmentalization within the pigeon basal ganglia. *Journal of Chemical Neuroanatomy*, *78*, 65–86. https://doi.org/10.1016/j.jchemneu.2016.08.005

Bupesh, M., Legaz, I., Abellán, A., Medina, L. (2011). Multiple telencephalic and extratelencephalic embryonic domains contribute neurons to the medial extended amygdala. *The Journal of Comparative Neurology*, *519*(8), 1505–1525. https://doi.org/10.1002/cne.22581

Butler, A. B., Reiner, A., & Karten, H. J. (2011). Evolution of the amniote pallium and the origins of mammalian neocortex. *Annals of the New York Academy of Sciences*, *1225*, 14–27. https://doi.org/10.1111/j.1749-6632.2011.06006.x

Campanella, L. C., da Silva, A. A., Gellert, D. S., Parreira, C., Ramos, M. C., Paschoalini, M. A., & Marino-Neto, J. (2009). Tonic serotonergic control of ingestive behaviours in the pigeon (*Columba livia*): The role of the arcopallium. *Behavioural Brain Research*, *205*(2), 396–405. https://doi.org/10.1016/j.bbr.2009.07.017

Casini, G., Bingman, V. P., & Bagnoli, P. (1986). Connections of the pigeon dorsomedial forebrain studied with WGA-HRP and 3H-proline. *The Journal of Comparative Neurology*, *245*(4), 454–470. https://doi.org/10.1002/cne.902450403

Chen, C. C., Winkler, C. M., Pfenning, A. R., & Jarvis, E. D. (2013). Molecular profiling of the developing avian telencephalon: Regional timing and brain subdivision continuities. *Journal of Comparative Neurology*, *521*(16), 3666–3701. https://doi.org/10.1002/cne.23406

Cheng, M., Chaiken, M., Zuo, M., & Miller, H. (1999). Nucleus taenia of the amygdala of birds: Anatomical and functional studies in ring doves (*Streptopelia risoria*) and European starlings (*Sturnus vulgaris*). *Brain, Behavior and Evolution*, *53*(5–6), 243–270. https://doi.org/6597

Cohen, D. H. (1975). Involvement of the avian amygdalar homologue (archistriatum posterior and mediale) in defensively conditioned heart rate change. *The Journal of Comparative Neurology*, *160*(1), 13–35. https://doi.org/10.1002/cne.901600103

Cremer, C. M., Bidmon, H. J., Gorg, B., Palomero-Gallagher, N., Escobar, J. L., Speckmann, E. J., & Zilles, K. (2010). Inhibition of glutamate/glutamine cycle in vivo results in decreased benzodiazepine binding and differentially regulated GABAergic subunit expression in the rat brain. *Epilepsia*, *51*(8), 1446–1455. https://doi.org/EPI2562 [pii]10.1111/j.1528-1167.2010.02562.x

Cremer, C. M., Palomero-Gallagher, N., Bidmon, H. J., Schleicher, A., Speckmann, E. J., & Zilles, K. (2009). Pentylenetetrazole-induced seizures affect binding site densities for GABA, glutamate and adenosine receptors in the rat brain. *Neuroscience*, *163*(1), 490–499. https://doi.org/S0306-4522(09)00454-0[pii]10.1016/j.neuroscience.2009.03.068

Cross, D. J., Marzluff, J. M., Palmquist, I., Minoshima, S., Shimizu, T., & Miyaoka, R. (2013). Distinct neural circuits underlie assessment of a diversity of natural dangers by American crows. *Proceedings of the Royal Society*, *280*(1765), 20131046. https://doi.org/10.1098/rspb.2013.1046

da Silva, A. A., Campanella, L. C., Ramos, M. C., Parreira, C., Faria, M. S., Marino-Neto, J., & Paschoalini, M. A. (2009). Arcopallium, NMDA antagonists and ingestive behaviors in pigeons. *Physiology & Behavior*, *98*(5), 594–601. https://doi.org/10.1016/j.physbeh.2009.09.009

Dafters, R. (1975). Active avoidance behavior following archistriatal lesions in pigeons. *Journal of Comparative and Physiological Psychology*, *89*(10), 1169–1179.

de Lanerolle, N. C., Elde, R. P., Sparber, S. B., & Frick, M. (1981). Distribution of methionine-enkephalin immunoreactivity in the chick brain: An immunohistochemical study. *The Journal of Comparative Neurology*, *199*(4), 513–533. https://doi.org/10.1002/cne.901990406

De Olmos, J. S., & Ingram, W. R. (1972). The projection field of the stria terminalis in the rat brain. An experimental study. *The Journal of Comparative Neurology*, *146*(3), 303–334. https://doi.org/10.1002/cne.901460303

Deviche, P., & Güntürkün, O. (1992). Peptides for calling? An immunohistochemical study of the avian n. intercollicularis. *Brain Research*, *569*(1), 93–99.

Diez-Alarcia, R., Pilar-Cuellar, F., Paniagua, M. A., Meana, J. J., & Fernandez-López, A. (2006). Pharmacological characterization and

autoradiographic distribution of alpha2-adrenoceptor antagonist [3H] RX 821002 binding sites in the chicken brain. *Neuroscience*, *141*(1), 357–369. https://doi.org/10.1016/j.neuroscience.2006.03.025

Dugas-Ford, J., Rowell, J. J., & Ragsdale, C. W. (2012). Cell-type homologies and the origins of the neocortex. *Proceedings of the National Academy of Sciences of the United States of America*, *109*(42), 16974–16979. https://doi.org/10.1073/pnas.1204773109

Edinger, L. (1896). *Vorlesungen über den Bau der nervœsen Centralorgane des Menschen und der Tiere für Ärzte und Studierende* (5., stark verm. Aufl. ed.). Leipzig: Vogel.

Edinger, L. (1903). *5 Untersuchungen über das Vorderhirn der Vögel*.

Fernandez-Lopez, A., Revilla, V., Candelas, M. A., Gonzalez-Gil, J., Diaz, A., & Pazos, A. (1997). A comparative study of alpha2- and beta-adrenoceptor distribution in pigeon and chick brain. *The European Journal of Neuroscience*, *9*(5), 871–883.

Gallyas, F. (1971). A principle for silver staining of tissue elements by physical development. *Acta Morphologica Academiae Scientiarum Hungaricae*, *19*(1), 57–71.

Gati, G., Lendvai, D., Hokfelt, T., Harkany, T., & Alpar, A. (2014). Revival of calcium-binding proteins for neuromorphology: Secretagogin typifies distinct cell populations in the avian brain. *Brain, Behavior and Evolution*, *83*(2), 82–92. https://doi.org/10.1159/000357834

Gebhard, R., Zilles, K., Schleicher, A., Everitt, B. J., Robbins, T. W., & Divac, I. (1995). Parcellation of the frontal cortex of the New World monkey Callithrix jacchus by eight neurotransmitter-binding sites. *Anatomy and Embryology*, *191*(6), 509–517.

Geyer, S., Matelli, M., Luppino, G., Schleicher, A., Jansen, Y., Palomero-Gallagher, N., & Zilles, K. (1998). Receptor autoradiographic mapping of the mesial motor and premotor cortex of the macaque monkey. *The Journal of Comparative Neurology*, *397*(2), 231–250. https://doi.org/10.1002/(SICI)1096-9861(19980727)397:2<231::AID-CNE6>3.0.CO;2-1 [pii]

Graebenitz, S., Kedo, O., Speckmann, E. J., Gorji, A., Panneck, H., Hans, V., … Pape, H. C. (2011). Interictal-like network activity and receptor expression in the epileptic human lateral amygdala. *Brain*, *134*(Pt 10), 2929–2947. https://doi.org/10.1093/brain/awr202

Güntürkün, O., & Bugnyar, T. (2016). Cognition without Cortex. *Trends in Cognitive Sciences*, *20*(4), 291–303. https://doi.org/10.1016/j.tics.2016.02.001

Hanics, J., Teleki, G., Alpar, A., Szekely, A. D., & Csillag, A. (2016). Multiple amygdaloid divisions of arcopallium send convergent projections to the nucleus accumbens and neighboring subpallial amygdala regions in the domestic chicken: A selective pathway tracing and reconstruction study. *Brain Structure & Function*, *222*, 301–315. https://doi.org/10.1007/s00429-016-1219-8

Herold, C., Bingman, V. P., Strockens, F., Letzner, S., Sauvage, M., Palomero-Gallagher, N., … Güntürkün, O. (2014). Distribution of neurotransmitter receptors and zinc in the pigeon (*Columba livia*) hippocampal formation: A basis for further comparison with the mammalian hippocampus. *Journal of Comparative Neurology*, *522*(11), 2553–2575. https://doi.org/10.1002/cne.23549

Herold, C., Coppola, V. J., & Bingman, V. P. (2015). The maturation of research into the avian hippocampal formation: Recent discoveries from one of the nature's foremost navigators. *Hippocampus*, *25*(11), 1193–1211. https://doi.org/10.1002/hipo.22463

Herold, C., Diekamp, B., & Güntürkün, O. (2008). Stimulation of dopamine D1 receptors in the avian fronto-striatal system adjusts daily cognitive fluctuations. *Behavioural Brain Research*, *194*(2), 223–229. https://doi.org/10.1016/j.bbr.2008.07.017

Herold, C., Joshi, I., Chehadi, O., Hollmann, M., & Güntürkün, O. (2012). Plasticity in D1-like receptor expression is associated with different components of cognitive processes. *PLoS One*, *7*(5), e36484. https://doi.org/10.1371/journal.pone.0036484

Herold, C., Palomero-Gallagher, N., Günturkün, O., & Zilles, K. (2012). Serotonin 5-HT(1A) receptor binding sites in the brain of the pigeon (*Columba livia*). *Neuroscience*, *200*, 1–12. https://doi.org/S0306-4522(11)01259-0 [pii]10.1016/j.neuroscience.2011.10.050

Herold, C., Palomero-Gallagher, N., Hellmann, B., Kröner, S., Theiss, C., Güntürkün, O., & Zilles, K. (2011). The receptor architecture of the pigeons' nidopallium caudolaterale: An avian analogue to the mammalian prefrontal cortex. *Brain Structure and Function*, *216*(3), 239–254. https://doi.org/10.1007/s00429-011-0301-5

Husband, S. A., & Shimizu, T. (1999). Efferent projections of the ectostriatum in the pigeon (*Columba livia*). *The Journal of Comparative Neurology*, *406*(3), 329–345.

Jarvis, E. D., Güntürkün, O., Bruce, L., Csillag, A., Karten, H., Kuenzel, W., … Avian Brain Nomenclature, C. (2005). Avian brains and a new understanding of vertebrate brain evolution. *Nature Reviews. Neuroscience*, *6*(2), 151–159. https://doi.org/10.1038/nrn1606

Jarvis, E. D., Yu, J., Rivas, M. V., Horita, H., Feenders, G., Whitney, O., … Wada, K. (2013). Global view of the functional molecular organization of the avian cerebrum: Mirror images and functional columns. *Journal of Comparative Neurology*, *521*(16), 3614–3665. https://doi.org/10.1002/cne.23404

Karten, H., & Hodos, W. (1967). *A stereotaxic atlas of the brain of the pigeon (Columba livia)*. Baltimore: The Johns Hopkins University Press.

Karten, H. J. (2015). Vertebrate brains and evolutionary connectomics: On the origins of the mammalian 'neocortex'. *Philosophical Transactions of the Royal Society of London. Series B, Biological Sciences*, *370*(1684), https://doi.org/10.1098/rstb.2015.0060

Kohler, E. C., Messer, W. S., Jr., & Bingman, V. P. (1995). Evidence for muscarinic acetylcholine receptor subtypes in the pigeon telencephalon. *The Journal of Comparative Neurology*, *362*(2), 271–282. https://doi.org/10.1002/cne.903620209

Kröner, S., & Güntürkün, O. (1999). Afferent and efferent connections of the caudolateral neostriatum in the pigeon (*Columba livia*): A retro- and anterograde pathway tracing study. *Journal of Comparative Neurology*, *407*(2), 228–260. https://doi.org/10.1002/(SICI)1096-9861(19990503)407:2<228::AID-CNE6>3.0.CO;2-2 [pii]

Kubikova, L., Wada, K., & Jarvis, E. D. (2010). Dopamine receptors in a songbird brain. *The Journal of Comparative Neurology*, *518*(6), 741–769. https://doi.org/10.1002/cne.22255

Kuenzel, W. J., Medina, L., Csillag, A., Perkel, D. J., & Reiner, A. (2011). The avian subpallium: New insights into structural and functional subdivisions occupying the lateral subpallial wall and their embryological origins. *Brain Research*, *1424*, 67–101. https://doi.org/10.1016/j.brainres.2011.09.037

Lanuza, E., Davies, D. C., Landete, J. M., Novejarque, A., & Martinez, G., F. (2000). Distribution of CGRP-like immunoreactivity in the chick and quail brain. *The Journal of Comparative Neurology*, *421*(4), 515–532.

Letzner, S., Simon, A., & Güntürkün, O. (2016). Connectivity and neurochemistry of the commissura anterior of the pigeon (*Columba livia*). *The Journal of Comparative Neurology*, *524*(2), 343–361. https://doi.org/10.1002/cne.23858

Leutgeb, S., Husband, S., Riters, L. V., Shimizu, T., & Bingman, V. P. (1996). Telencephalic afferents to the caudolateral neostriatum of the pigeon. *Brain Research*, *730*(1–2), 173–181. https://doi.org/0006-8993(96)00444-1 [pii]

Lillethorup, T. P., Iversen, P., Fontain, J., Wegener, G., Doudet, D. J., & Landau, A. M. (2015). Electroconvulsive shocks decrease alpha2-adrenoceptor binding in the Flinders rat model of depression.

European Neuropsychopharmacology, *25*(3), 404–412. https://doi.org/10.1016/j.euroneuro.2014.12.003

Lovell, P. V., Clayton, D. F., Replogle, K. L., & Mello, C. V. (2008). Birdsong "transcriptomics": Neurochemical specializations of the oscine song system. *PLoS One*, *3*(10), e3440. https://doi.org/10.1371/journal.pone.0003440

Martinez-Vargas, M. C., Stumpf, W. E., & Sar, M. (1976). Anatomical distribution of estrogen target cells in the avian CNS: A comparison with the mammalian CNS. *The Journal of Comparative Neurology*, *167*(1), 83–103. https://doi.org/10.1002/cne.901670106

Mash, D. C., & Potter, L. T. (1986). Autoradiographic localization of M1 and M2 muscarine receptors in the rat brain. *Neuroscience*, *19*(2), 551–564.

Medina, L., & Abellán, A. (2009). Development and evolution of the pallium. *Seminars in Cell & Developmental Biology*, *20*(6), 698–711. https://doi.org/10.1016/j.semcdb.2009.04.008

Medina, L., Bupesh, M., & Abellán, A. (2011). Contribution of genoarchitecture to understanding forebrain evolution and development, with particular emphasis on the amygdala. *Brain, Behavior and Evolution*, *78*(3), 216–236. https://doi.org/10.1159/000330056

Merker, B. (1983). Silver staining of cell bodies by means of physical development. *Journal of Neuroscience Methods*, *9*(3), 235–241.

Montiel, J. F., & Molnar, Z. (2013). The impact of gene expression analysis on evolving views of avian brain organization. *The Journal of Comparative Neurology*, *521*(16), 3604–3613. https://doi.org/10.1002/cne.23403

Moreno, N., & Gonzalez, A. (2007). Evolution of the amygdaloid complex in vertebrates, with special reference to the anamnio-amniotic transition. *Journal of Anatomy*, *211*(2), 151–163. https://doi.org/10.1111/j.1469-7580.2007.00780.x

Mulder, J., Spence, L., Tortoriello, G., Dinieri, J. A., Uhlen, M., Shui, B., … Harkany, T. (2010). Secretagogin is a Ca2+-binding protein identifying prospective extended amygdala neurons in the developing mammalian telencephalon. *European Journal of Neuroscience*, *31*(12), 2166–2177. https://doi.org/10.1111/j.1460-9568.2010.07275.x

Nomura, T., Hattori, M., & Osumi, N. (2009). Reelin, radial fibers and cortical evolution: insights from comparative analysis of the mammalian and avian telencephalon. *Development, Growth & Differentiation*, *51*(3), 287–297. https://doi.org/10.1111/j.1440-169X.2008.01073.x

Olson, C. R., Hodges, L. K., & Mello, C. V. (2015). Dynamic gene expression in the song system of zebra finches during the song learning period. *Developmental Neurobiology*, *75*(12), 1315–1338. https://doi.org/10.1002/dneu.22286

Palomero-Gallagher, N., Vogt, B. A., Schleicher, A., Mayberg, H. S., Zilles, K. (2009). Receptor architecture of human cingulate cortex: evaluation of the four-region neurobiological model. *Human Brain Mapping*, *30*(8), 2336–2355. https://doi.org/10.1002/hbm.20667

Palomero-Gallagher, N., Schleicher, A., Zilles, K., & Loscher, W. (2010). The circling ci2 rat mutant revisited: Receptor architecture of the motor cortex. *Neuroscience*, *170*(2), 542–550. https://doi.org/10.1016/j.neuroscience.2010.07.043

Palomero-Gallagher, N., & Zilles, K. (2004). Isocortex. In G. Paxinos (ed), *The rat nervous system* (3rd ed., pp. 729–757). San Diego: Acadamic Press.

Palomero-Gallagher, N., Zilles, K., Schleicher, A., & Vogt, B. A. (2013). Cyto- and receptor architecture of area 32 in human and macaque brains. *The Journal of Comparative Neurology*, *521*(14), 3272–3286. https://doi.org/10.1002/cne.23346

Paxinos, G., Kus, L., Ashwell, K., & Watson, C. (1999). *Chemoarchitecture of the rat forebrain*. San Diego: Academic Press.

Paxinos, G., & Watson, C. (2005). *The Rat Brain in Stereotaxic Coordinates*. Elsevier Academic Press.

Pfenning, A. R., Hara, E., Whitney, O., Rivas, M. V., Wang, R., Roulhac, P. L., … Jarvis, E. D. (2014). Convergent transcriptional specializations in the brains of humans and song-learning birds. *Science*, *346*(6215), 1256846. https://doi.org/10.1126/science.1256846

Puelles, L. (2011). Pallio-pallial tangential migrations and growth signaling: new scenario for cortical evolution? *Brain, Behavior and Evolution*, *78*(1), 108–127. https://doi.org/10.1159/000327905

Puelles, L., Kuwana, E., Puelles, E., Bulfone, A., Shimamura, K., Keleher, J., … Rubenstein, J. L. (2000). Pallial and subpallial derivatives in the embryonic chick and mouse telencephalon, traced by the expression of the genes Dlx-2, Emx-1, Nkx-2.1, Pax-6, and Tbr-1. *The Journal of Comparative Neurology*, *424*(3), 409–438.

Puelles, L., Martinez-de-la-Torre, M., Paxinos, G., Watson, C., & Martinez, S. (2007). *The chick brain in stereotaxic coordinates: An Atlas featuring neuromeric subdivisions and mammalian homologies*. London: Academic Press.

Puelles, L., Medina, L., Borello, U., Legaz, I., Teissier, A., Pierani, A., & Rubenstein, J. L. (2015). Radial derivatives of the mouse ventral pallium traced with Dbx1-LacZ reporters. *Journal of Chemical Neuroanatomy*, *75*(Pt A), 2–19 https://doi.org/10.1016/j.jchemneu.2015.10.011

Reiner, A., & Karten, H. J. (1985). Comparison of olfactory bulb projections in pigeons and turtles. *Brain, Behavior and Evolution*, *27*(1), 11–27.

Reiner, A., Perkel, D. J., Bruce, L. L., Butler, A. B., Csillag, A., Kuenzel, W. … Avian Brain Nomenclature Forum. (2004). Revised nomenclature for avian telencephalon and some related brainstem nuclei. *The Journal of Comparative Neurology*, *473*(3), 377–414. https://doi.org/10.1002/cne.20118

Roberts, T. F., Hall, W. S., & Brauth, S. E. (2002). Organization of the avian basal forebrain: Chemical anatomy in the parrot (*Melopsittacus undulatus*). *The Journal of Comparative Neurology*, *454*(4), 383–408. https://doi.org/10.1002/cne.10456

Sah, P., Faber, E. S., Lopez De Armentia, M., & Power, J. (2003). The amygdaloid complex: Anatomy and physiology. *Physiological Reviews*, *83*(3), 803–834. https://doi.org/10.1152/physrev.00002.2003

Saint-Dizier, H., Constantin, P., Davies, D. C., Leterrier, C., Levy, F., & Richard, S. (2009). Subdivisions of the arcopallium/posterior pallial amygdala complex are differentially involved in the control of fear behaviour in the Japanese quail. *Brain Research Bulletin*, *79*(5), 288–295. https://doi.org/10.1016/j.brainresbull.2009.03.004

Sanders, J. D., Szot, P., Weinshenker, D., Happe, H. K., Bylund, D. B., & Murrin, L. C. (2006). Analysis of brain adrenergic receptors in dopamine-beta-hydroxylase knockout mice. *Brain Research*, *1109*(1), 45–53. https://doi.org/10.1016/j.brainres.2006.06.033

Scarf, D., Stuart, M., Johnston, M., & Colombo, M. (2016). Visual response properties of neurons in four areas of the avian pallium. *Journal of Comparative Physiology. A, Neuroethology, Sensory, Neural, and Behavioral Physiology*, *202*(3), 235–245. https://doi.org/10.1007/s00359-016-1071-6

Schall, U., Güntürkün, O., & Delius, J. D. (1986). Sensory projections to the nucleus basalis prosencephali of the pigeon. *Cell and Tissue Research*, *245*(3), 539–546.

Scheperjans, F., Grefkes, C., Palomero-Gallagher, N., Schleicher, A., & Zilles, K. (2005). Subdivisions of human parietal area 5 revealed by quantitative receptor autoradiography: A parietal region between motor, somatosensory, and cingulate cortical areas. *Neuroimage*, *25*(3), 975–992. https://doi.org/10.1016/j.neuroimage.2004.12.017

Scheperjans, F., Palomero-Gallagher, N., Grefkes, C., Schleicher, A., & Zilles, K. (2005). Transmitter receptors reveal segregation of cortical areas in the human superior parietal cortex: Relations to visual and somatosensory regions. *Neuroimage*, *28*(2), 362–379. https://doi.org/10.1016/j.neuroimage.2005.06.028

Shanahan, M., Bingman, V. P., Shimizu, T., Wild, M., & Güntürkün, O. (2013). Large-scale network organization in the avian forebrain: A connectivity matrix and theoretical analysis. *Frontiers in Computational Neuroscience*, *7*, 89. https://doi.org/10.3389/fncom.2013.00089

Sun, Z., & Reiner, A. (2000). Localization of dopamine D1A and D1B receptor mRNAs in the forebrain and midbrain of the domestic chick. *Journal of Chemical Neuroanatomy*, *19*(4), 211–224.

Swanson, L. W. (2000). Cerebral hemisphere regulation of motivated behavior. *Brain Research*, *886*(1–2), 113–164.

Swanson, L. W., & Petrovich, G. D. (1998). What is the amygdala? *Trends in Neurosciences*, *21*(8), 323–331.

Székély, A. D., & Krebs, J. R. (1996). Efferent connectivity of the hippocampal formation of the zebra finch (Taenopygia guttata): An anterograde pathway tracing study using Phaseolus vulgaris leucoagglutinin. *Journal of Comparative Neurology*, *368*(2), 198–214. https://doi.org/10.1002/(SICI)1096-9861(19960429)368:2<198::AID-CNE3>3.0.CO;2-Z [pii]10.1002/(SICI)1096-9861(19960429)368:2<198::AID-CNE3>3.0.CO;2-Z

Thompson, R. R., Goodson, J. L., Ruscio, M. G., & Adkins-Regan, E. (1998). Role of the archistriatal nucleus taeniae in the sexual behavior of male Japanese quail (Coturnix japonica): A comparison of function with the medial nucleus of the amygdala in mammals. *Brain, Behavior and Evolution*, *51*(4), 215–229.

Veenman, C. L., Wild, J. M., & Reiner, A. (1995). Organization of the avian "corticostriatal" projection system: A retrograde and anterograde pathway tracing study in pigeons. *The Journal of Comparative Neurology*, *354*(1), 87–126. https://doi.org/10.1002/cne.903540108

Vicario, A., Abellán, A., Desfilis, E., & Medina, L. (2014). Genetic identification of the central nucleus and other components of the central extended amygdala in chicken during development. *Frontiers in Neuroanatomy*, *8*, 90. https://doi.org/10.3389/fnana.2014.00090

Vicario, A., Abellán, A., & Medina, L. (2015). Embryonic origin of the Islet1 and Pax6 neurons of the chicken central extended amygdala using cell migration assays and relation to different neuropeptide-containing cells. *Brain, Behavior and Evolution*, *85*(3), 139–169. https://doi.org/10.1159/000381004

Vogt, B. A., Hof, P. R., Zilles, K., Vogt, L. J., Herold, C., & Palomero-Gallagher, N. (2013). Cingulate area 32 homologies in mouse, rat, macaque and human: Cytoarchitecture and receptor architecture. *The Journal of Comparative Neurology*, *521*(18), 4189–4204. https://doi.org/10.1002/cne.23409

Wada, K., Sakaguchi, H., Jarvis, E. D., & Hagiwara, M. (2004). Differential expression of glutamate receptors in avian neural pathways for learned vocalization. *The Journal of Comparative Neurology*, *476*(1), 44–64. https://doi.org/10.1002/cne.20201

Wang, R., Chen, C. C., Hara, E., Rivas, M. V., Roulhac, P. L., Howard, J. T., … Jarvis, E. D. (2015). Convergent differential regulation of SLIT-ROBO axon guidance genes in the brains of vocal learners. *The Journal of Comparative Neurology*, *523*(6), 892–906. https://doi.org/10.1002/cne.23719

Whitney, O., Pfenning, A. R., Howard, J. T., Blatti, C. A., Liu, F., Ward, J. M., … Jarvis, E. D. (2014). Core and region-enriched networks of behaviorally regulated genes and the singing genome. *Science*, *346*(6215), 1256780. https://doi.org/10.1126/science.1256780

Wild, J. M., Arends, J. J., & Zeigler, H. P. (1984). A trigeminal sensorimotor circuit for pecking, grasping and feeding in the pigeon (*Columba livia*). *Brain Research*, *300*(1), 146–151.

Wild, J. M., Arends, J. J., & Zeigler, H. P. (1985). Telencephalic connections of the trigeminal system in the pigeon (*Columba livia*): A trigeminal sensorimotor circuit. *The Journal of Comparative Neurology*, *234*(4), 441–464. https://doi.org/10.1002/cne.902340404

Wild, J. M., Arends, J. J., & Zeigler, H. P. (1990). Projections of the parabrachial nucleus in the pigeon (*Columba livia*). *The Journal of Comparative Neurology*, *293*(4), 499–523. https://doi.org/10.1002/cne.902930402

Wild, J. M., Karten, H. J., & Frost, B. J. (1993). Connections of the auditory forebrain in the pigeon (*Columba livia*). *The Journal of Comparative Neurology*, *337*(1), 32–62. https://doi.org/10.1002/cne.903370103

Winkowski, D. E., & Knudsen, E. I. (2007). Top-down control of multimodal sensitivity in the barn owl optic tectum. *The Journal of Neuroscience*, *27*(48), 13279–13291. https://doi.org/10.1523/JNEUROSCI.3937-07.2007

Wynne, B., & Güntürkün, O. (1995). Dopaminergic innervation of the telencephalon of the pigeon (*Columba livia*): A study with antibodies against tyrosine hydroxylase and dopamine. *Journal of Comparative Neurology*, *357*(3), 446–464. https://doi.org/10.1002/cne.903570309

Yamamoto, K., & Reiner, A. (2005). Distribution of the limbic system-associated membrane protein (LAMP) in pigeon forebrain and midbrain. *The Journal of Comparative Neurology*, *486*(3), 221–242. https://doi.org/10.1002/cne.20562

Yamamoto, K., Sun, Z., Wang, H. B., & Reiner, A. (2005). Subpallial amygdala and nucleus taeniae in birds resemble extended amygdala and medial amygdala in mammals in their expression of markers of regional identity. *Brain Research Bulletin*, *66*(4–6), 341–347. https://doi.org/10.1016/j.brainresbull.2005.02.016

Yilmazer-Hanke, D. M., Roskoden, T., Zilles, K., & Schwegler, H. (2003). Anxiety-related behavior and densities of glutamate, GABAA, acetylcholine and serotonin receptors in the amygdala of seven inbred mouse strains. *Behavioural Brain Research*, *145*(1–2), 145–159.

Zeier, H., & Karten, H. J. (1971). The archistriatum of the pigeon: Organization of afferent and efferent connections. *Brain Research*, *31*(2), 313–326.

Zilles, K. (2005). Evolution of the human brain and comparative cyto- and receptor architecture. In S. Dehaene, J.-R. Duhamel, M. Hauser, & G. Rizzolatti (Eds), *From monkey brain to human brain* (pp. 41–56). Cambridge: MIT Press.

Zilles, K., & Palomero-Gallagher, N. (2016). Comparative analysis of receptor subtypes that identify primary cortical sensory areas. In J. Kaas, G. Striedter, L. Krubitzer, S. Herculano-Houzel, & T. Preuss (Eds.), *Evolution of the nervous system*. Oxford: Elsevier.

Zilles, K., Palomero-Gallagher, N., Grefkes, C., Scheperjans, F., Boy, C., Amunts, K., & Schleicher, A. (2002). Architectonics of the human cerebral cortex and transmitter receptor fingerprints: Reconciling functional neuroanatomy and neurochemistry. *European Neuropsychopharmacology*, *12*(6), 587–599. https://doi.org/S0924977X02001086 [pii]

Zilles, K., Palomero-Gallagher, N., & Schleicher, A. (2004). Transmitter receptors and functional anatomy of the cerebral cortex. *Journal of Anatomy*, *205*(6), 417–432. https://doi.org/10.1111/j.0021-8782.2004.00357.x

Zilles, K., Schlaug, G., Matelli, M., Luppino, G., Schleicher, A., Qu, M., … Roland, P. E. (1995). Mapping of human and macaque sensorimotor areas by integrating architectonic, transmitter receptor, MRI and PET data. *Journal of Anatomy*, *187*(Pt 3), 515–537.

Zilles, K., Schleicher, A., Palomero-Gallagher, N., & Amunts, K. (2002). Quantitative analysis of cyto- and receptor architecture of thehuman brain. In J.C. Mazziotta & A. Toga (Eds.), *Brain mapping: The methods* (pp. 573–602). Amsterdam: Elsevier.

How to cite this article: Herold C, Paulitschek C, Palomero-Gallagher N, Güntürkün O, Zilles K. Transmitter receptors reveal segregation of the arcopallium/amygdala complex in pigeons (*Columba livia*). *J Comp Neurol*. 2018;526:439–466. https://doi.org/10.1002/cne.24344